Contents

Front cover

The new T799 representation of European orography and examples of global gridpoint resolution.

Supporting WMO Members

The recent ECMWF Council held in July decided to enhance the set of ECMWF products disseminated to WMO Members. The improvement will be quite significant and includes:

◆ An extension of the forecast range of the products distributed on the GTS to day 10 for several parameters.

◆ The provision of global products from the Ensemble Prediction System (EPS) in support of high impact and extreme weather. This includes in particular the Extreme Forecast Index (EFI) for wind, precipitation and temperature (see ECMWF Newsletter No. 107).

◆ The provision of site-specific forecast products (namely EPSgrams) at selected locations, specifically targeting synoptic stations in developing countries, especially the least developed ones (on average 5–10 per country). This follows a recommendation made in 2005 by the WMO Executive Council. The list of sites will be prepared in consultation with WMO.

The support from ECMWF to WMO Members stems directly from the Centre's Convention which states that one of the Centre's objectives shall be "to assist in implementing programmes of the World Meteorological Organization". In 1988, less than ten years after it started issuing operational forecasts, the Centre was designated as a Regional/ Specialised Meteorological Centre of WMO, specialising in global medium-range weather forecasts. At the same time it was also designated as the monitoring centre for upper-air observations. Since then this support has been consistently developed over the years by the ECMWF Council, in recognition of its duties to the wider meteorological community, especially toward developing countries.

The support provided to WMO Members concerns specifically early warnings of severe weather and monitoring of the observing system. The main enhancements introduced in recent years have been the addition of tropical cyclone forecasts, the provision of global seasonal forecasts and the development of real-time monitoring of satellite data. As for the priority given to supporting developing countries, it is significant to note that, at its last session, the ECMWF Council also agreed the provision of products to the African Centre for Meteorological Applications for Development (ACMAD), the Centro Internacional para la Investigacion del Fenomeno de El Niño (CIIFEN) and the Bangladesh Flood Forecasting Project.

All these new products will be added to the website which ECMWF has recently developed for WMO Members. This site provides, amongst other things, the latest medium-range forecasts together with documentation about ECMWF products available on the GTS and from data servers. It also provides free decoding software for downloading. This site is accessible by going to the ECMWF home page at www.ecmwf.int, and then clicking on the WMO icon. Access to the forecast products is password protected and the password is provided to the National Meteorological Service of a country upon request of that country's Permanent Representative to WMO.

Dominique Marbouty

Changes to the operational forecasting system

David Richardson

Changes to the operational forecasting system

There have been no changes to the operational forecasting system since the last issue of the ECMWF Newsletter.

Planned changes

The testing of a new model cycle continues. The new version includes the following.

◆ Revisions and changes to the cloud scheme including treatment of ice supersaturation and new numerics.
◆ Implicit computation of convective transports.
◆ Introduction of turbulent orographic form drag scheme and revision to sub-grid scale orographic drag scheme.
◆ Gust fix for orography and stochastic physics.
◆ Revised assimilation of rain-affected radiances.
◆ Variational bias correction of satellite radiances.

Technical changes in preparation for the extension of the EPS to day 15 at reduced resolution (VAREPS) are also included.

New items on the ECMWF web site

Andy Brady

Verification of monthly forecast

This site provides some information on the quality and consistency of the ECMWF monthly forecasts. Weekly mean anomalies computed using ECMWF's operational analysis for a given week are compared with the four monthly forecasts starting one week apart and verifying on that week. The time range of the forecasts is days 5–11 for the most recent forecast, days 12–18, days 19–25 and days 26–32.

www.ecmwf.int/products/forecasts/d/charts/mofc/verification/

MJO Products

Products that describe the Madden-Julian Oscillation (MJO) activity as predicted by the monthly forecast are now available. The MJO, also known as the 40-day wave, is a large-scale oscillation (wave) in the equatorial region. The MJO originates over the Indian Ocean and travels east at 800 km per day (10 ms^{-1}).

www.ecmwf.int/products/forecasts/d/charts/mofc/forecast/mjo/

12th Workshop on the Use of High Performance Computing in Meteorology

Every second year the ECMWF hosts a workshop on the use of high performance computing in meteorology. The emphasis of this workshop will be on running meteorological applications at sustained teraflops performance in a production environment, and on the application specific developments required to move towards petaflops computing. This year the workshop is planned for 30 October to 3 November 2006.

www.ecmwf.int/newsevents/meetings/workshops/2006/high_performance_computing-12th/

ECMWF/GEO Reanalysis Workshop Presentations

Presentations are available from the ECMWF/GEO Workshop on Atmospheric Re-analysis which took place from 19 to 22 June at ECMWF. This workshop considered the status of and plans global reanalysis in Europe, Japan and the USA.

www.ecmwf.int/newsevents/meetings/workshops/2006/re-analysis/

ENSEMBLES Project Meeting Presentations

Presentations are available from the ENSEMBLES Joint RT1 and RT2A Meeting which was held at ECMWF on 8–9 June. The Research Themes RT1 and RT2A deal with the generation and production of the global ensemble integrations for seasonal, decadal and longer timescales. The meeting considered the status of these integrations, the goals achieved to date and the plans for the third year of the project.

www.ecmwf.int/newsevents/meetings/workshops/2006/ensembles/

Thorpex Interactive Grand Global Ensemble (TIGGE) web site

TIGGE is a key component of THORPEX: a World Weather Research Programme to accelerate the improvements in the accuracy of 1-day to 2-week forecasts of high-impact weather for the benefit of humanity.

http://tigge.ecmwf.int/

ECMWF's contribution to EUMETSAT's H-SAF

Matthias Drusch, Erik Andersson, Peter Bauer, Philippe Bougeault

Satellite Application Facilities (SAFs) are specialised development and processing centres within the EUMETSAT Applications Ground Segment. Conceptually, the SAF network complements the production of standard meteorological products derived from satellite data at EUMETSAT in Darmstadt. There are currently eight SAFs out of which five are in initial operations and three are under development. The 'Support to Operational Hydrology
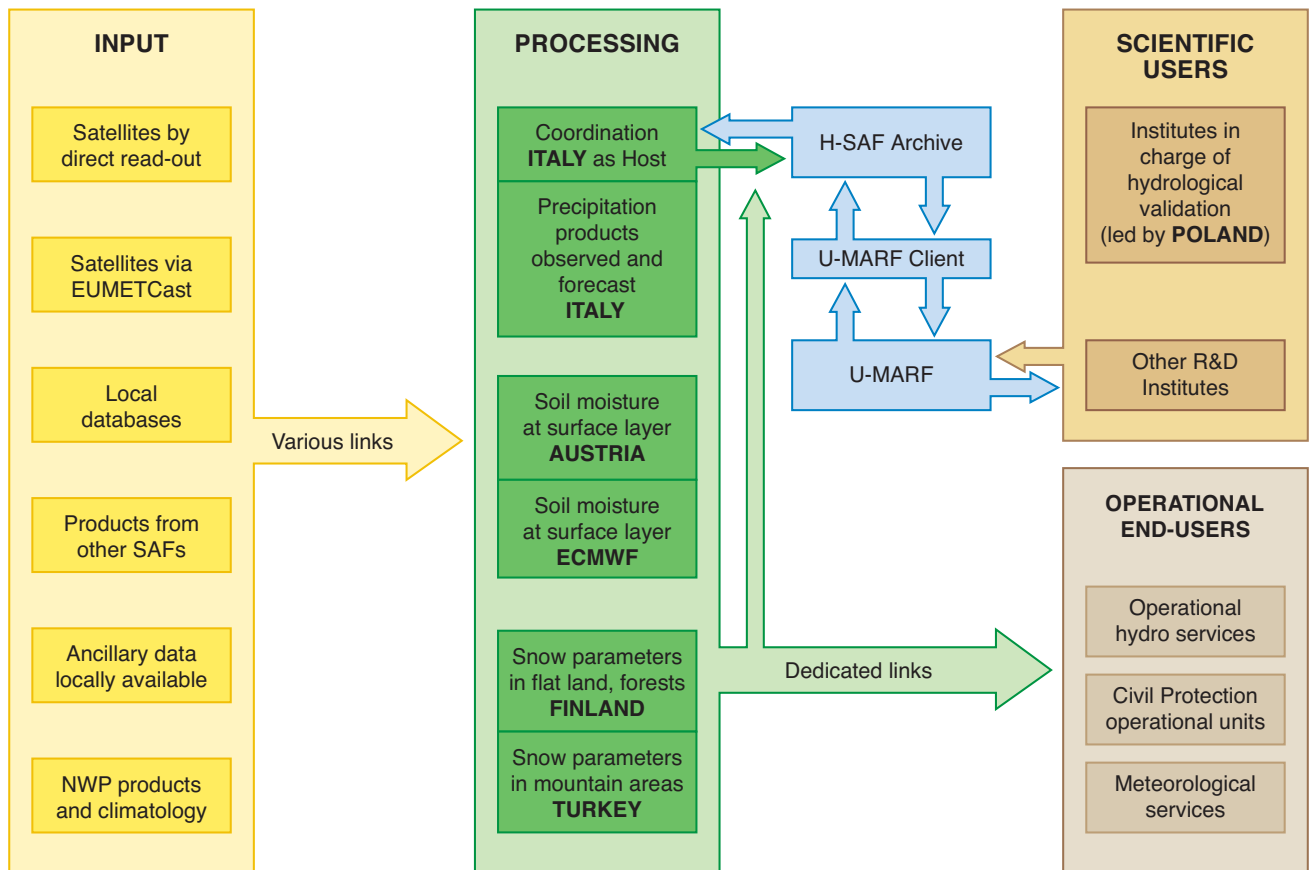
System architecture of H-SAF (from the H-SAF Project Plan).

and Water Management' SAF (H-SAF) was approved by EUMETSAT Council in June 2004 and the five-year development phase started on 1 September 2005.

The H-SAF is hosted by the Italian Met Service and its main objectives are:

◆ To provide new satellite-derived products for the geographical area of Europe from existing and future satellites with sufficient time and space resolution to satisfy the needs for operational hydrology. The three core parameters are precipitation (liquid, solid, rate, cumulate; cluster leader: Italian Met Service), soil moisture (at the surface and in the root zone; cluster leader: Zentral Anstalt für Meteorologie und Geodynamik, Austria), and snow (cover, melting conditions, snow water equivalent; cluster leader: Finish Meteorological Institute).

◆ To perform independent validation of the usefulness of the new products for minimizing the impact of floods, landslides, and avalanches and evaluating water resources. The work in this hydrology cluster (leader: Institute of Meteorology and Water Management, Poland) comprises downscaling/upscaling modelling from large-scale fields to catchment level, observation data fusion (e.g. satellite derived products, radar measurements, raingauge networks), and data impact studies for hydrological applications. ECMWF is a contributor to the core soil moisture product and is represented in the H-SAF Steering Group and the Project Team. ECMWF's main activity is the development of a root zone soil moisture product based on satellite derived top-level surface soil moisture and the operational modelled first guess of soil moisture for the top 1 m soil layer. It is envisaged to use a surface analysis scheme based on an extended Kalman filter, which has been developed and tested within the framework of the European Land Data Assimilation Study (ELDAS). This system has not yet been used operationally and will be implemented within the framework of this project.

The prototype development for the root zone soil moisture product will be based on surface soil moisture derived from the scatterometers onboard the European Remote Sensing Satellites (ERS-1/2). This global data set has been made available by Vienna University for the period covering 1992 to 2001. The final operational H-SAF product will rely on observations from the Advanced Scatterometer (ASCAT) onboard MetOp. Preparatory work for this near real time product was carried out in EUMETSAT's Numerical Weather Prediction (NWP) SAF. Within the framework of the precipitation cluster ECMWF will explore the possibilities of retrieving and assimilating rain from Special Sensor Microwave/Imager (SSM/I) and Special Sensor Microwave Imager/Sounder (SSMIS) observations over land.

Further information about the H-SAF can be found by going to www.eumetsat.int and following the link from "WHAT WE DO".

Book about the predictability of weather and climate

Philippe Bougeault

The topic of predictability in weather and climate has advanced significantly in recent years, both in understanding the phenomena that affect predictability of weather and climate and in techniques used to model and forecast predictability. To review these developments a seminar on "*Predictability of Weather and Climate*" was held at ECMWF in September 2002, with presentations covering the whole range of theoretical and practical aspects on weather and climate timescales. Topics such as the predictability of weather phenomena, coupled land-ocean-atmosphere systems and anthropogenic climate change were amongst those included. Also ensemble systems for forecasting predictability were covered.

Because of the comprehensive and authoritative nature of the presentations it was decided to publish an updated and expanded version of the proceedings. The book "*Predictability of Weather and Climate*", edited by Tim Palmer and Renate Hagedorn, has now been published by Cambridge University Press. Included in the book are contributions dealing with:

◆ Theoretical/mathematical aspects of predictability theory.
◆ Data assimilation and predictability.
◆ Predictability of different timescales and phenomena.
◆ Operational ensemble forecasting systems.
◆ Use of predictability in decision-making processes.

There are no less than 29 chapters and much, much more than in the Seminar Proceedings.

The texts and figures are of high quality, and I thank all ECMWF colleagues who helped in the preparation of this landmark volume.

Several of the leading experts in NWP and climate have summarized years of their experience and most profound thinking about the fundamental questions of our discipline. I anticipate that this is going to become a classic on our shelves and will be used for a very long time.

For more information go to: www.cambridge.org/uk/catalogue/catalogue.asp?isbn=0521848822
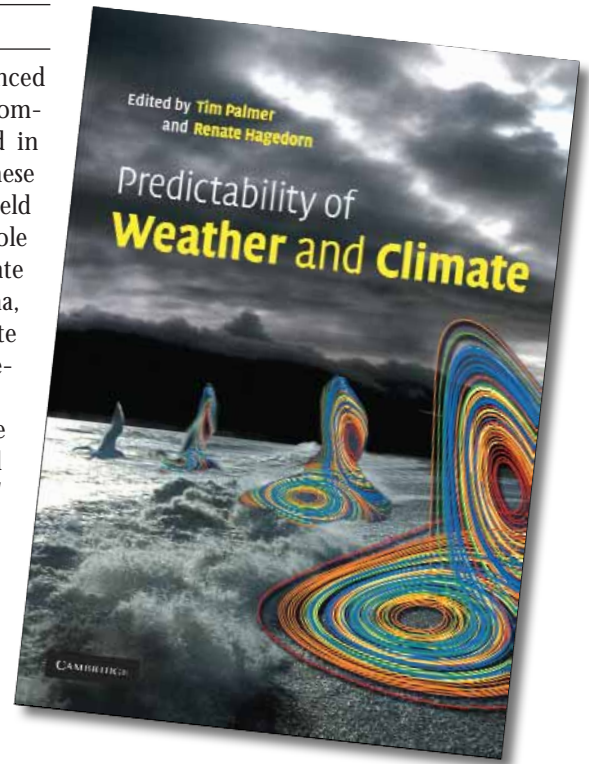
65th Council session on 6–7 July 2006

Manfred Kloeppel

At the invitation of its President, Anton Eliassen from Norway, the ECMWF Council held its 65th session in Oslo on 6–7 July 2006. The main results of this session were as follows.

◆ *Co-operation Agreements*. The Director was authorised to conclude an agreement with Morocco for scientific and technical co-operation.

◆ *Financial Matters*. The Council took note of the Auditor's Report regarding the financial year 2005 and gave discharge to the Director in respect of the implementation of the budget for 2005. The Council adopted amendments to the Financial Regulations of the Centre which will improve the overall management of the Centre's Budget.

◆ *Pensions*. The Council agreed to allow consultants from Member States and Co-operating States with an uninterrupted contract exceeding two years to enrol in the Centre's Funded Pension Scheme.

◆ *High Performance Computing Requirements*. The Council took note of the Centre's High Performance Computing requirements and, in order to address various challenges (requirements regarding high performance computing, pensions, and increasing electricity costs) agreed to set up a Task Team to consider long-term funding solutions.

◆ *Products of the Centre*. The Council agreed to add some products to the catalogue of ECMWF real-time products. It also agreed to the reduction of Information Charges for small service providers. It approved the enhancement of product dissemination for WMO Members, in particular with regard to supporting high impact and extreme weather event forecasting (e.g. the global Extreme Forecast Index for wind, precipitation and temperature).

The Council supported the Centre's engagement with the GEO (Group on Earth Observation) initiative, and agreed that ECMWF, on request by GEO, would provide data sets specifically linked to GEO activities (e.g. reanalysis, DEMETER and observing system studies) or data sets derived from 24 GHz impact studies.

Participants at the 65th ECWMF Council session in Oslo (courtesy of Detlev Frömming, Deutscher Wetterdienst).

The Council agreed that ECMWF's digital seasonal forecast products be provided to CIIFEN (Centro International para la Investigatión del Fenómeno de El Niño) for use in research and development for a period of three years. It was also agreed by Council that the Centre's medium-range and seasonal forecast products be provided to the Bangladesh Meteorological Department for official duty flood forecasts in Bangladesh.

A celebration of the career of David Anderson

Philippe Bougeault

A special meeting was held at ECMWF on 23 June 2006 to celebrate the career of David Anderson, who retires as Head of the Seasonal Forecast Section later this year. During the day, a workshop in honour of David was held – people came from all over the world to participate. Talks were given by world leaders in the fields of oceanography and meteorology, some of whom were ex-students of David. In the evening a gala dinner was held with speeches and live music. The event, organized by David's colleagues, was very successful, and I would like to thank in particular Magdalena Balmaseda, Tim Palmer and Alberto Troccoli from ECMWF, and Keith Haines from University of Reading.

David obtained his PhD from St Andrews University, and has held positions at CSIRO Australia, Department of Applied Maths, Cambridge, and the Department of Atmospheric, Oceanic and Planetary Physics, Oxford. During this period David established his reputation as a world-class physical oceanographer, working on the dynamics of ocean circulations in the tropics and extratropics. With Jay McCreary, he developed one of the first coupled models to explain the El Niño phenomenon.

David had a sabbatical at ECMWF to work on scatterometer data in the mid 1980s, but finally became Head of the Seasonal Forecast Section in 1995. Under David's leadership ECMWF has developed a seasonal forecast system which is second to none in the world. As well as providing forecasts for our Member States, ECMWF seasonal forecasts are now used for a number of humanitarian applications in health and hydrology in developing countries.

In addition, David made many contributions to the international organisation of climate science. He contributed to the early stages of WOCE, and was involved in the TOGA programme throughout its lifetime, including serving as chairman of the international scientific steering group for several years Also he served as co-vice chair of the CLIVAR programme during its development phase.

On behalf of David's many friends and colleagues from around the world I wish him a very happy retirement including success in whatever ventures beckon beyond ECMWF!

Norbert Gerbier Mumm International Award

Philippe Bougeault

The Norbert Gerbier Mumm International Award recognises an original scientific paper on the influence of meteorology in a particular field of the physical, natural or human sciences, or on the influence of one of these sciences on meteorology. The award aims to stimulate interest in such research in support of WMO programmes.

The Award for 2006 goes to Tim Palmer and his DEME-TER team (which includes Renate Hagedorn and Francisco Doblas-Reyes from ECMWF) for their paper entitled "Development of a European Multimodel Ensemble System for Seasonal-to-Interannual Prediction (DEMETER)" which appeared in the *Bulletin of the American Meteorological Society*, 2004, **85**, 853–872. The DEMETER team consists of 25 scientists from twelve institutions within Europe and one in the USA. Congratulations to all!

The DEMETER system comprises seven global atmospheric-ocean coupled models running from an ensemble of initial conditions. The paper describes a comprehensive evaluation of a set of hindcasts and provides evidence that the multimodel ensemble approach is more skilful than using a single-model ensemble for the seasonal time-scale. In addition examples are given of the application of seasonal ensemble forecasts to malaria and crop yield prediction. These examples illustrate the value of seasonal-to-interannual prediction to the economy and society as a whole.

More information about the EU-funded DEMETER project can be found at: www.ecmwf.int/research/demeter

Andy Morse (University of Liverpool), Francisco Doblas-Reyes, Tim Palmer and Renate Hagedorn (ECMWF) after having received the Norbert Gerbier Mumm International Award on behalf of the DEMETER Team at a ceremony in Geneva on 28 June.

The results of this multidisciplinary investigation not only confirm the promising developments carried out in dynamical seasonal ensemble forecasting, but also demonstrates the value of climate forecasts, giving the scientists the motivation to explore new avenues for realising the full potential of our forecasts for real end-user applications. An important operational follow-up of DEMETER is the EUROSIP project, whereby seasonal forecasts from ECMWF, the Met Office and Météo-France are brought together in a single multi-model ensemble. It is expected that more contributors will join in the future.

Towards a global meso-scale model:
The high-resolution system T799L91 and T399L62 EPS

Agathe Untch, Martin Miller, Mariano Hortal,
Roberto Buizza, Peter Janssen

On 1 February 2006, a major resolution upgrade of the operational ECMWF forecasting systems was successfully implemented as IFS Cycle 30r1. This article describes the main components of this change, their rationale, and expected impacts and benefits. It should be noted, however, that many people at ECMWF other than the authors of this article have contributed to the scientific development work for this high-resolution system and the results presented here.

Increases in horizontal and vertical resolution of the Centre's global model and assimilation system have been a cornerstone of the long-term development plans, and during its history have contributed major improvements to the forecast skill at all time ranges. The 25 years or so of the Centre's operational activities have seen four significant horizontal resolution changes with a similar number of changes in the

vertical resolution also. Each change to higher resolution has been based on realistic expectations of improved accuracy in (a) the representation of basic components such as orography and land/sea definition, (b) synoptic and sub-synoptic systems, (c) weather features and parameters such as fronts, cloud and rain bands, jets, and (d) assimilating observations both space-based and surface-based. Also, the later refinements in resolution have brought systematic improvements to the ocean wave forecasts, not least in their quality near coastlines and in confined waters (typical of the European region) which particularly benefit from more accurate surface winds. In general, these changes have been well received by users and have also contributed significantly to the long-term positive trends in objective measures of forecast skill. They are also visible in a variety of other forecast verification exercises such as those carried out by WGNE (*Ebert et al.*, 2003) for precipitation and tropical cyclone tracking.

Before 1 February, the ECMWF operational resolution of T511 (grid spacing ~ 40 km) accurately resolved systems

of only several hundred kilometres. It was clear that use of a higher resolution (e.g. 25 km) should improve both the description of important structures within active synoptic weather systems and provide opportunities to capture the true intensity of the highly energetic mesoscale systems associated with many severe weather events. The modelling of fine-scale filament-like potential vorticity features often associated with such events has been discussed by a number of authors (e.g. *Dritschel et al.*, 1999).

The representativeness of observations has always been an important issue in data assimilation and continues to be so. What is clear however is that the more accurate the assimilating model the more useful the observation can be. Hence a higher resolution assimilating model has several advantages in this regard: it can use low-level data better (due to more accurate orography etc.) and has a greater likelihood of representing the observed parameter since it can describe more accurately the local horizontal and vertical structures in that parameter. This is also the case for remotely sensed observations, many of which have much higher resolutions than are currently handled by assimilation systems that severely thin or sub-sample the data.

The resolution of the Ensemble Prediction System (EPS) has changed twice before: from T63L19 to T159L31 in December 1996, and then to T255L40 in November 2000. These upgrades were implemented following extensive experimentation that showed that the resolution improvement was beneficial, as confirmed by subsequent operational experience.

Resolution and severe weather prediction

The majority of severe weather events are notable for either their local nature or for more local features embedded in somewhat larger-scale phenomena. It is therefore obvious that resolution is a crucial issue in capturing the nature and intensity of such events. Our ability to forecast severe weather is partly limited by the inherent unpredictability of the phenomena in question, and partly by the forecast skill of the large-scale patterns with which they are associated. The recent marked improvements in forecast skill both in the early medium-range and beyond are an important step forward in this regard (e.g. *Grazzini*, 2005). Furthermore, whether it is through improved detail in surface forcing, improved use of observations or through improved dynamics and physics of the mesoscales, higher resolutions are a key driving factor in improving the accuracy in the prediction of severe weather (both at ECMWF and other NWP Centres). Examples of this can be found in *Miller* (1999).

The new high-resolution deterministic system T799L91

Horizontal resolution increase

The horizontal resolution of the deterministic system has been increased from T511 to T799. The ECMWF model is a spectral model, and horizontal resolution is denoted by the highest wavenumber represented in the model. The notation T799 means that the highest wavenumber represented with the new resolution is 799. This corresponds to a wavelength of 50 km. The smallest wavelength represented in the previous operational resolution T511 is 78 km. In the above notation 'T' stands for 'triangular spectral truncation'.

In gridpoint space, the linear Gaussian grid corresponding to the new T799 resolution has 800 latitude rows, an increase by 288 rows from the T511 grid (512 latitude rows). Along each latitude row near the equator there are 1,600 grid-points in the new resolution. This number decreases gradually for latitudes approaching the poles since a 'reduced'
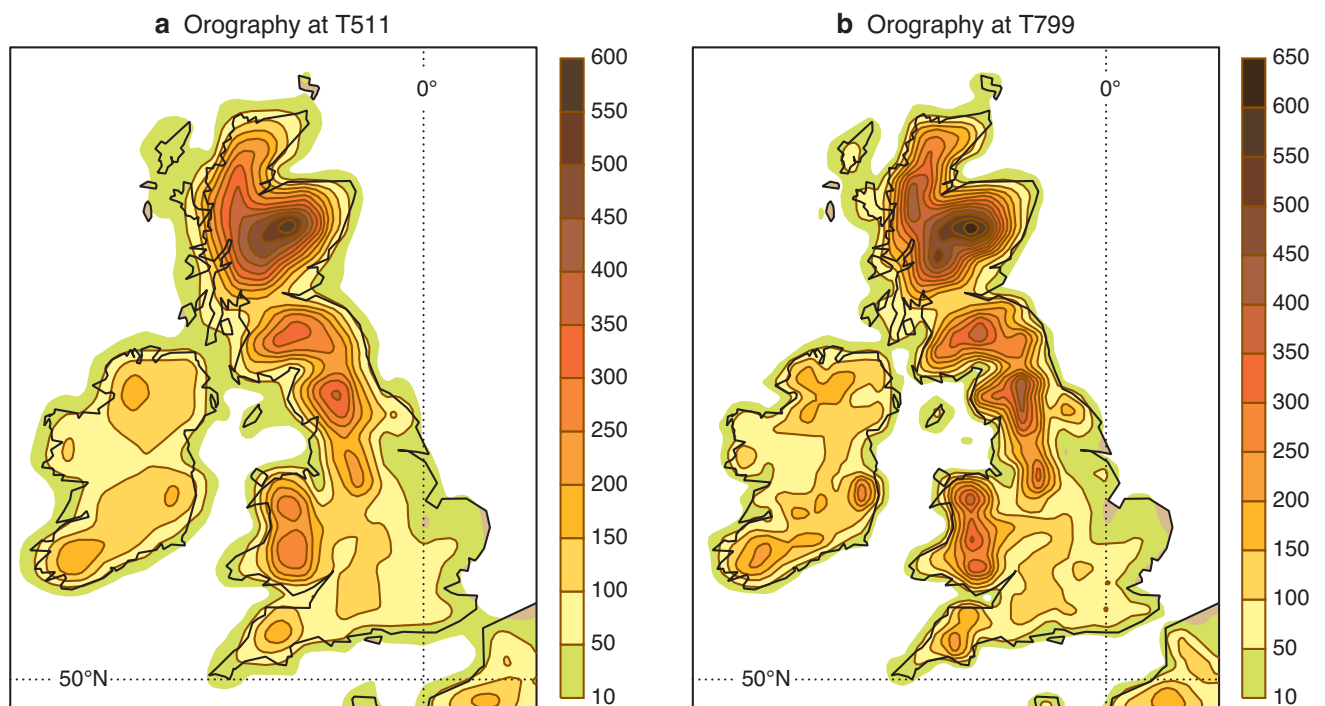
Figure 1 Orography at (a) horizontal resolutions T511 (grid spacing ~ 40 km) and (b) T799 (grid spacing ~ 25 km).

Gaussian grid is used in the ECMWF model. In total, the new horizontal grid has 843,490 grid-points, 494,962 more than the T511 grid (348,528 grid-points in total). This corresponds to a 2.42 fold increase in the number of grid-points per vertical level.

Figure 1 shows the orography for the British Isles at T511 and at T799. The coast lines in the higher resolution model follow much more closely the shape of the real coast lines. For the hilly areas of the U.K. and Ireland, the increase in orographic detail and realism with T799 is noteworthy. As is well-recognized, this improvement in the representation of the orography leads directly to improved forecasts of weather events which are strongly influenced by orographic features.

In the 4D-Var assimilation, the outer loops also change to T799 while the horizontal resolution of the second inner loop has been upgraded from T159 to T255. The first inner loop resolution remains unchanged at T95.

Vertical resolution increase

Concurrent with the horizontal resolution increase the vertical resolution of the deterministic model has been upgraded. The deterministic 10-day forecast and the analysis use now 91 vertical levels (previously 60 levels).

In the new 91-level resolution (L91), and depending on latitude and season, approximately 45–50 of the 91 levels are located in the troposphere. The remaining 40–45 levels resolve the stratosphere and mesosphere up to an altitude of about 80 km (0.01 hPa). Figure 2 shows the distribution of levels in L91 compared to the previous operational 60-level distribution (L60). The vertical resolution has increased every-

where in the atmosphere compared to L60. However, the largest increase is around the tropopause, where the resolution has nearly doubled. The model top has been raised from 0.1 hPa (~64 km) to 0.01 hPa (~80 km) partly to create a deeper sponge layer for wave absorption, but also to provide the basis for a possible future replacement of Rayleigh friction by parametrized non-orographic gravity wave drag. Currently a simple Rayleigh friction is applied to the zonal wind in layers above 5 hPa to slow down the otherwise excessively strong polar night jets at the stratopause level.

Time step decrease

Whenever the model resolution is increased numerical stability constraints usually force a reduction in the length of the time step which can be safely used. However, with a semi-implicit semi-Lagrangian time stepping scheme, as used in the ECMWF model, the stability constraints are not very strict. Nevertheless, mainly for accuracy reasons, the time step for the T799L91 model was decreased from 15 minutes as used with the T511L60 resolution to 12 minutes. The time step in the second inner loop of 4D-Var was kept at 30 minutes although the resolution was increased from T159L60 to T255L91.

Resolution increase in the coupled ocean wave model

In tandem with the increase in horizontal and vertical resolution of the IFS, resolution in the ocean wave prediction model was increased as well. For the deterministic forecast the spatial resolution was increased from 0.5° to 0.36°. A further increase from 0.36° to the nominal atmospheric resolution of 0.25° is not needed, because the smallest scale
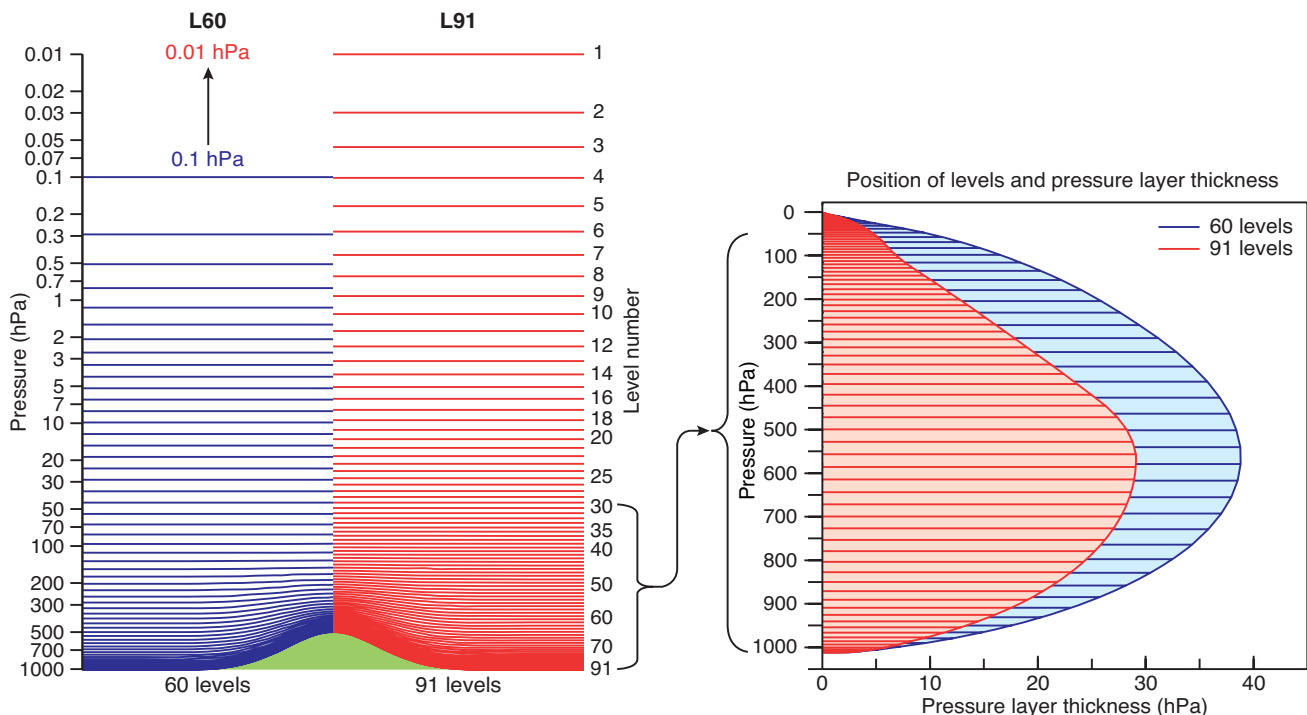
Figure 2 The left-hand panel shows the distribution of vertical levels in the L60-model (purple) and L91-model (red). The right-hand side panel shows the position of the levels in the troposphere with the length of each horizontal bar indicating the thickness of the layer centred about the corresponding level.

features in the atmospheric model are heavily damped. Also experiments with matching atmospheric and ocean wave resolution have shown that there is no additional gain in information on ocean waves or atmospheric parameters. To facilitate a coupling between the wind and waves every atmospheric model time step, the advection and wave physics time step was reduced from 15 to 12 min. However, the ocean wave model is only responsible for about 5% of the total forecast CPU time. No modifications to the source term formulation were required.

The T399L62 high-resolution EPS

The resolution of the ECMWF Ensemble Prediction System was also increased. The main differences between the new and the old system are the following.

◆ *Forecast model resolution*: T399L62 (30 min time step) used instead of T255L40.

◆ *Initial perturbations resolution*: Perturbations are generated using T42L62 instead of T42L40 singular vectors.

◆ *Initial perturbation amplitude*: The contribution to the amplitudes of the initial perturbations generated using the 48-hour evolved singular vectors has been decreased by approximately 30% (this change was needed to compensate for the faster growth of the T42L62 initial perturbations when non-linearly integrated in the T399L62 model).

Like the previous 40-level model, the new 62-level model for the EPS is primarily a 'troposphere only model' with the top at ~5 hPa and with only a few levels in the stratosphere. In the troposphere (up to about 200 hPa), the distribution of levels in L62 is identical to the L91 distribution. Both the ensemble size (50 perturbed and one unperturbed member) and the forecast length (10 days) have been kept the same. This resolution change is part of the upgrading process that will lead to the implementation of the Variable Resolution Ensemble Prediction System (VAREPS), designed to extend the forecast range covered by the ensemble system initially to 15 days and eventually to 32 days, through the merging of the medium-range and monthly ensemble prediction systems. See the article by *Buizza et al.* in this Newsletter for more details.

For the ensemble prediction of ocean waves, spectral resolution was increased from 25 frequencies and 12 directions to 30 frequencies and 24 directions, and is now identical to the representation of the wave spectrum in the deterministic forecast. The EPS is an important tool for assessing the probability of the occurrence of extreme ocean wave conditions. Experience has shown that the increase in directional resolution was particularly beneficial for representing rapidly varying extreme conditions. No increase of spatial resolution (at the moment the ocean waves EPS has a resolution of 1°) was introduced for cost reasons, and because this was not really needed due to the lack of atmospheric variability at the small scales.

Cycle 30r1

In addition to the various resolution increases discussed above, there were several other important changes implemented.

◆ *Grid-point humidity and ozone in 4D-Var*: The analysis was changed such that humidity and ozone are no longer

required in spectral space in the inner loops of 4D-Var, thus eliminating errors in these fields resulting from the spectral transformations.

◆ *Ozone chemistry*: Revised coefficients (version 2.3) from Météo-France were used for the linearised ozone chemistry scheme of Cariolle and Déqué.

◆ *Wave information*: Additional wave height observations from the Jason Altimeter were introduced in the wave analysis while the SAR image spectra from ERS-2 (available every 200 km along track) were replaced by ASAR images from the ENVISAT satellite, available every 100 km.

Such a major upgrade in horizontal and vertical resolutions together with the changes listed above inevitably raised problems and issues during the extensive testing the new system underwent prior to operational implementation. Among the problems encountered were unphysical increments in the upper stratospheric and mesospheric humidity and a few cases of numerical instability in the inner loops of 4D-Var. Ways to alleviate these problems were found and included in Cy30r1, and ongoing research into these issues will deliver more elegant solutions in the near future.

Computational cost of the resolution increase

The 2.42 fold increase in the number of grid-points per vertical level, together with the increase in the number of vertical levels by 31 and the reduction in the time step to 12 minutes (from 15 minutes), led to a four fold increase in the total number of floating point operations necessary to complete a 10-day forecast: 1.7×10^{15} floating point operations at T799L91 as compared with 0.4×10^{15} at T511L60.

Figure 3 shows the relative cost contributions of the different parts of the model for the two resolutions. As was expected, the cost of the spectral transforms has grown faster with increased resolution than the rest of the model, but the spectral method is still very affordable. Tests with even higher horizontal resolutions (e.g. T2047) have shown that the spectral method will continue to remain affordable for the foreseeable future.

Area	Score	Day 2	Day 3	Day 5	Day 7
Northern Hemisphere	ACC	0.1%	2%	–	–
	RMSE	0.1%	0.1%	10%	–
Southern Hemisphere	ACC	0.1%	0.1%	0.1%	0.1%
	RMSE	0.1%	0.1%	0.1%	0.1%
Europe	ACC	–	–	2%	–
	RMSE	0.5%	2%	10%	5%

Table 1 The statistical significance obtained with the t-test for Z500 scores for Anomaly Correlation Coefficient (ACC) and Root Mean Square Error (RMSE) for the northern hemisphere, southern hemisphere and for Europe. Numbers in green cells mean the high-resolution system T799L91 (Cycle 30r1) is better than T511L60 (Cycle 29r2) with a statistical significance given by the value. Smaller values mean higher statistical significance. The sample size is 311 forecasts.
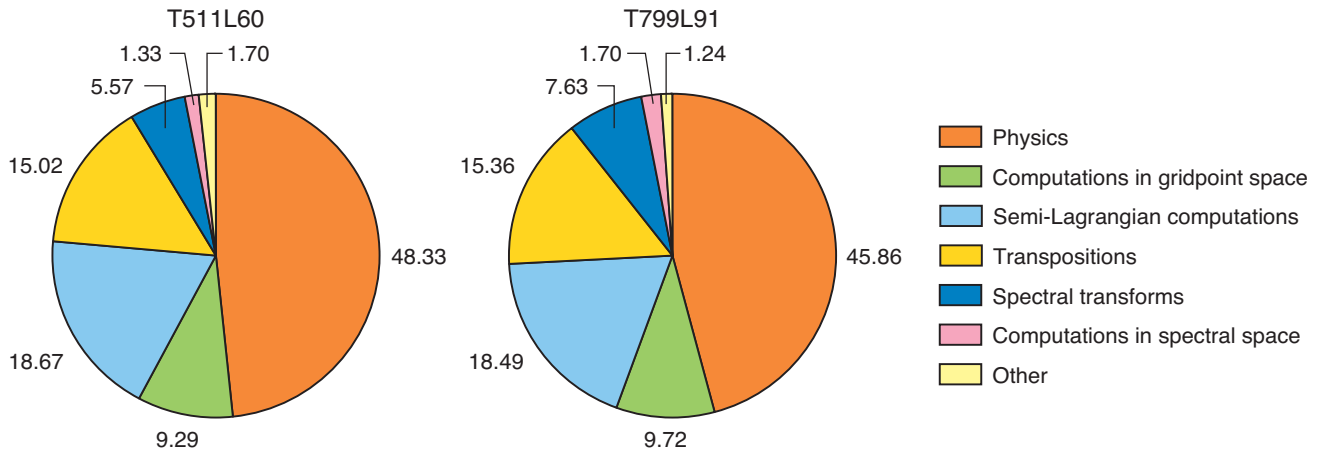
Figure 3 Pie charts showing the relative cost of various components of the model at T511L60 and T799L91 resolutions.

Performance of the high-resolution deterministic system

A total of ten months of assimilation-forecast experimentation were run with Cy30r1: four months (1 October 2005 to 31 January 2006) in experimental mode (e-suite 29) by the Operations Department and six months by the Research Department. The mean scores are in general better than the control scores with T511L60 and Cy29r2, with the largest gain and highest statistical significance in the southern hemisphere. Table 1 summarizes the statistical significance obtained with the t-test for Z500 scores for the northern hemisphere, southern hemisphere and for Europe.

Better representation of the orography and increased vertical resolution led to more observations being accepted in the analysis. As an example Figure 4 shows statistics on how many radiosonde temperature measurements are being accepted in the northern hemisphere and how well the background and analysis fit these observations in data assimilation with T799L91 and with T511L60 for the month of August 2005 (62 analysis cycles). The significant increase in

the number of observations accepted near the surface is due to the more realistic orography and coastlines, while the increase near the tropopause stems from the improvement in vertical resolution.

One severe weather example that occurred during the pre-operational testing of the high-resolution system is shown in Figure 5. Very strong onshore winds along the Norwegian coast on 12 December 2005, due to an intense polar low, caused surges along the coast and fjords. Comparison with the verifying analyses (left-hand side panels in Figure 5) shows that location and strength of the gale are much better captured with the new high-resolution system at the two forecast ranges of 3 and 5 days shown (middle and right-hand side panels in Figure 5, respectively).

As was anticipated, the enhanced resolution also has a positive effect on the quality of the forecasts of tropical cyclones, and both position and intensity errors are reduced in the high-resolution system at all forecast ranges. Hurricane Katrina, which devastated New Orleans in August 2005, was one of the strongest storms ever recorded in the Gulf of
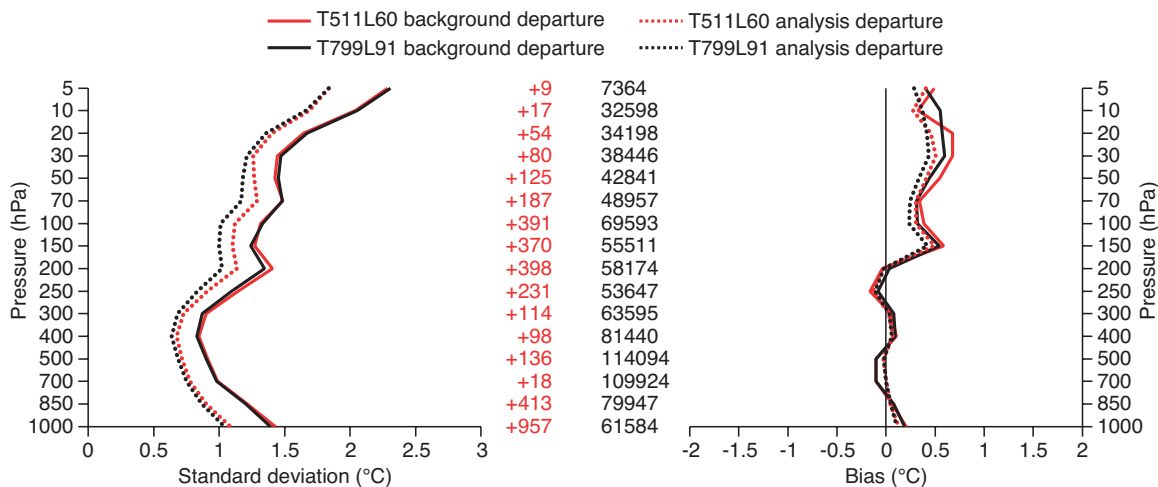
Figure 4 Fit of background and analysis to TEMP temperature observations in the northern hemisphere (averaged over 62 analysis cycles) in terms of standard deviation and bias: black lines T799L91, red lines T511L60. The numbers in black in the middle of the figure give the total number of TEMP temperature observations accepted by the T799L91 analysis per vertical band and the numbers in red give the difference in the number of observations used by the two analyses (a plus sign means more observations are accepted by the T799L91 analysis).

a T799L91
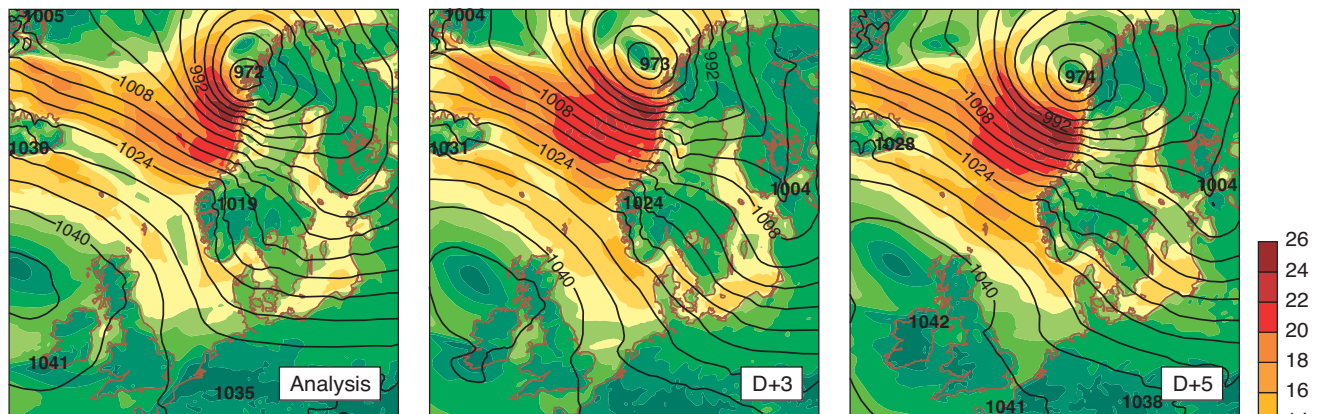
b T511L60
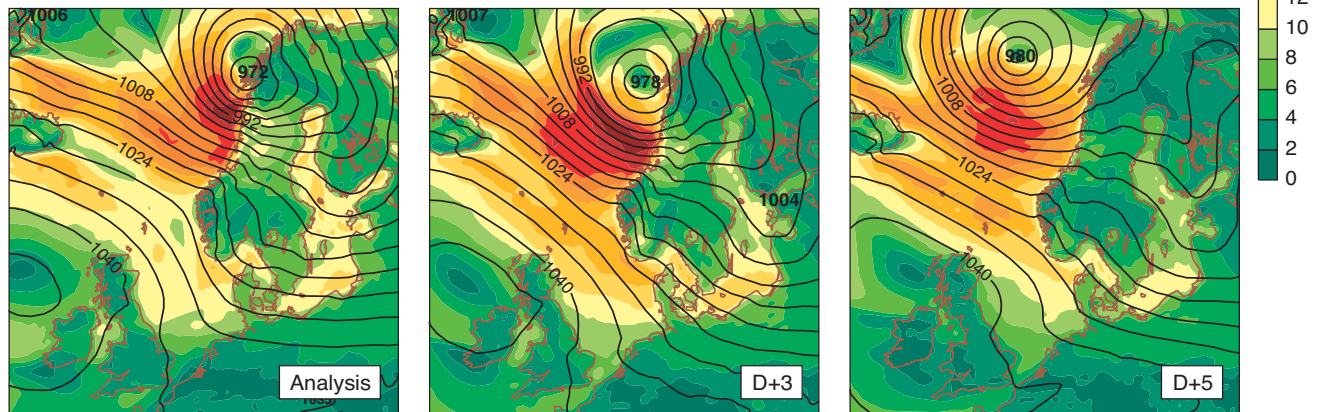
Figure 5 Mean sea level pressure and 10 m wind speed at 00 UTC on 12 December 2005 as analysed and predicted by (a) T799L91 and (b) T511L60: analysis (left), 3 day forecast (middle) and 5 day forecast (right).

Mexico (category 5), with maximum sustained winds of 280 km/h and a minimum central pressure of 902 hPa at its peak. By the time it made landfall on the Louisiana coast on 29 August it had decreased to a category 3 storm with a minimum central pressure of 920 hPa. Figure 6 compares the performance of the high-resolution and the T511L60 systems in forecasting this storm at landfall 36 h and 72 h in advance. Clearly, the high-resolution system captures position and intensity of the storm better at both forecast ranges. Note that the positive impact of increased resolution on the VAREPS forecast of Hurricane Katrina is considered in the companion article by *Buizza et al.* in this edition of the Newsletter.

Validation of the experimental suite for ocean waves against buoy data (located mainly in the northern hemisphere) shows small improvements in the scatter index of forecast wave height up to day 6 (see Figure 7).

Performance of the T399L62 EPS

The EPS performance for February, March and April (FMA) 2006 in predicting the 500 hPa geopotential height (Z500) over the northern hemisphere and Europe has been compared to its performance in the same period but for the previous three years, using a range of scores.

Results indicate that the new system has achieved the best performance of the past four FMA periods up to fore-cast day 7 with a better tuned ensemble spread, more skilful control and perturbed members, a more skilful ensemble-mean, and higher probabilistic scores.

On average in FMA 2006, the difference between the ensemble spread measured using the ensemble standard deviation, and the error of the ensemble-mean is the small-est up to forecast day 6 for the northern hemisphere (Figure 8(a)). During the same period, the ensemble-mean has an Anomaly Correlation Coefficient (ACC, computed with respect to the T799L91 analysis) above 0.6 out to day 10, and has a higher ACC than the ensemble control forecast and the high-resolution (T799L91) after day 3 (Figure 8(b)). It is noteworthy that the skill difference between the EPS control and the high-resolution system has decreased.

Probabilistic scores for the northern hemisphere for the same period using the area under the relative operating characteristic curve (which is a measure of the system to discriminate between hit and false alarm rates) show, for anomalies up to one climatological standard deviation, values greater than 0.75 up to forecast day 10 (Figure 9(a)). The Brier Skill Score (with the skill computed with respect to a climatological probabilistic prediction) for these thresh-olds is positive for the whole forecast range. Compared to the previous three years, the area under the relative oper-ating characteristic curve and the Brier Skill Score have the highest values (Figure 9(b)).
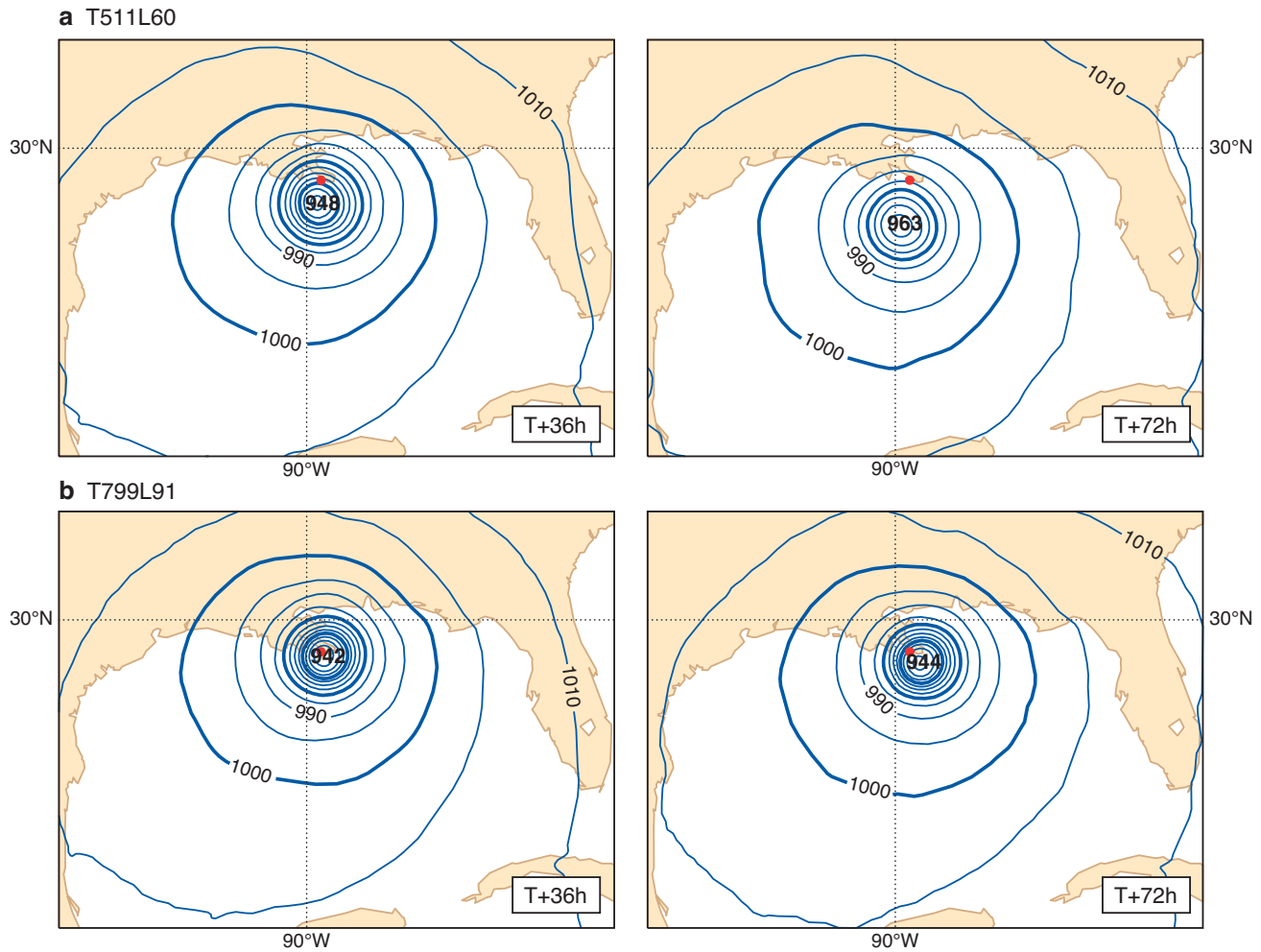
a T511L60

b T799L91

Figure 6 Forecasts of mean sea level pressure at 36 h and 72 h of hurricane Katrina for 12 UTC on 29 August 2005 using (a) T511L60 and (b) T799L91. The observed minimum pressure was 920 hPa at landfall, and the red dot marks the observed position of the cyclone.

What does the future hold?

There has been a particularly large improvement in operational forecasts over the past seven or so years, and evidence discussed here and elsewhere indicates that improvements have stemmed from improved data assimilation (improved assimilating models as well as improved analysis techniques), the availability of new or improved types of observation, refinements in physical processes, and from resolution increases across the entire forecast system.

In addition to the results presented here, forecasts of weather elements such as near-surface temperature, winds, cloud and precipitation have all improved. These benefit directly from model improvements as well as from the improved definition of the synoptic environment.

The spectral breakdown of error shows that there has been a distinct recent improvement in the handling of smaller scales of motion in the ECMWF system. In the new system's incremental 4D-Var data assimilation, the higher spectral truncation of the highest-resolution minimization is now at wavenumber 255. It has been shown previously that forecast error is still some way from saturation after twelve or even twenty-four hours for a range of wavenumbers higher than 159, making the case for further increasing the resolution of
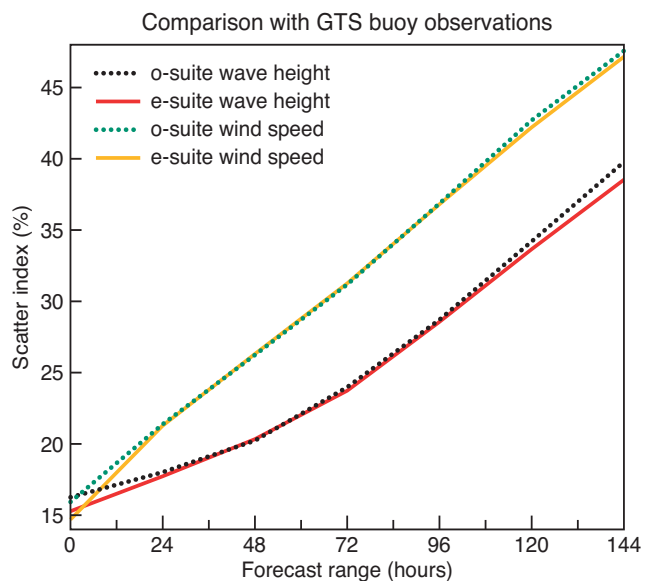
Figure 7 Comparison of scatter index (normalized standard deviation of error) in forecast wave height against buoy data between experimental suite (e-suite) and operational suite (o-suite). Period is from 1 October 2005 until 31 January 2006 and consists of 246 cases. The corresponding results for wind speed are shown as well.

a

b
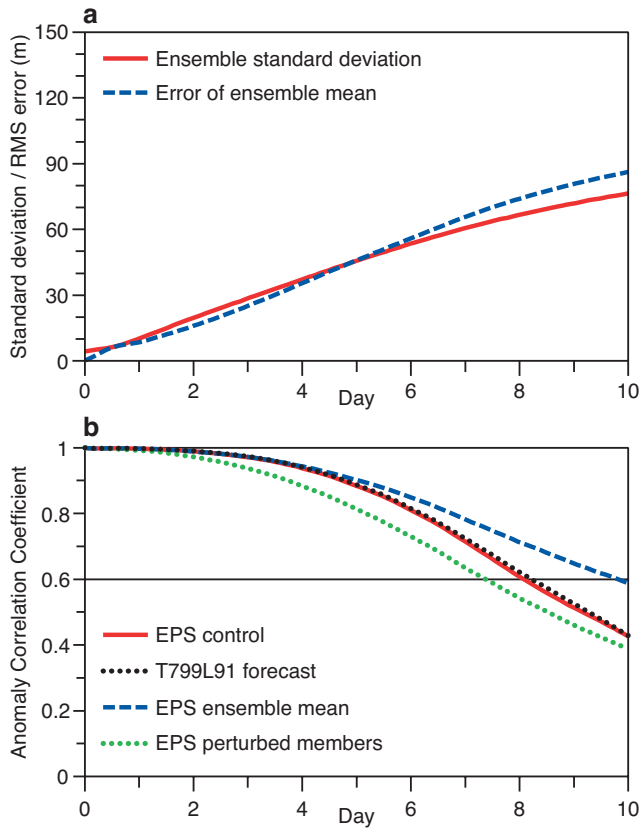
Figure 8 Average scores for Z500 over the northern hemisphere for February, March and April 2006. (a) Ensemble standard deviation and error of the ensemble-mean. (b) Anomaly Correlation Coefficient of the EPS control, T799L91 high-resolution forecast, EPS ensemble mean and the EPS perturbed members.

a

b

Figure 9 Spring average of Z500 over the northern hemisphere for (a) area under the relative operating characteristic curve for the prediction of positive Z500 anomalies and (b) Brier Skill Score (computed with respect to climatology) for 2006, 2005, 2004 and 2003.

the minimisation to produce more accurate initial conditions for the forecasts.

The refinements in resolution of the analysis and deterministic forecasts transfer their benefits to the Ensemble Prediction System both through the improved quality of the initial conditions and the fact that the EPS uses resolutions that have been previously well tested and efficiently configured.

Any discussion on future developments splits into what is planned under current constraints (e.g. computer budget) and what would be possible without. Realistically, the new forecast systems will provide a framework on which to progressively develop our analysis and forecasting capabilities during the next 4-5 years. This will undoubtedly lead to better forecast guidance at all ranges, as the assimilation algorithms, physical parametrizations and ensemble methods take advantage of the more accurate global model framework provided at these higher resolutions.

Much higher resolution tests of the IFS, at T1279 (15 km) and T2079 (10 km) suggest that with sufficient computer power such resolutions could be implemented with versions of our current numerics and physics. It is planned to implement

these resolutions operationally in 2010 and 2015 respectively, but the precise schedule will depend critically on the available budget for the high performance computing facility.

FURTHER READING

Buizza, **R.**, **J.-R. Bidlot**, **N. Wedi**, **M. Fuentes**, **M. Hamrud**, **G. Holt**, **T. Palmer** & **F. Vitart**, 2006: The ECMWF Variable Resolution Ensemble Prediction System (VAREPS). *ECMWF Newsletter No. 108*, 14–20.

Dritschel, **D.G.**, **L.M. Polvani** & **A.R. Mohebalhojeh**, 1999: The contour-advective semi-Lagrangian algorithm for the shallow water equations. *Mon. Wea. Rev.*, **127**, 1551–1565.

Ebert, **E.E.**, **U. Damrath**, **W. Wergen** & **M.E. Baldwin**, 2003: The WGNE assessment of short-term quantitative precipitation forecasts. *Bull. Am. Meteorol. Soc.*, **84**, 481–492.

Grazzini, **F**. 2005: The skill of the ECMWF forecasting system in the prediction of heavy rain events in the Alpine regions. *Submitted to Weather and Forecasting.*

Miller, **M.J.**, 1999: Resolution studies. *ECMWF Tech. Memo No. 299.*

The ECMWF Variable Resolution Ensemble Prediction System (VAREPS)

Roberto Buizza, Jean-Raymond Bidlot, Nils Wedi,
Manuel Fuentes, Mats Hamrud,
Graham Holt, Tim Palmer, Frederic Vitart

The Ensemble Prediction System (EPS) has been part of the ECMWF operational suite since December 1992. At that time, the EPS was based on 33 forecasts produced with a T63L19 (spectral triangular truncation T63 with 19 vertical levels) resolution version of the ECMWF model (*Molteni et al.*, 1996). The initial uncertainties were simulated by starting 32 members from perturbed initial conditions defined by T21L31 perturbations which are rapidly-growing during the first 36 hours of the forecast range (the singular vectors, see *Buizza & Palmer*, 1995).

Since December 1992, the EPS has been upgraded several times. During these years, the EPS has used the same model version as the data assimilation and forecast system, benefiting from all the changes made. Some of these changes included substantial modifications of the EPS configuration, designed to improve both the simulation of initial and model uncertainties. It is worth identifying a few of them.

◆ In 1994 the optimisation time interval of the singular vectors was extended to 48 hours.

◆ In 1995 the resolution of the singular vectors was increased to T42L31.

◆ In 1996 the system was upgraded to a 51-member T159L31 system (spectral triangular truncation T159 with linear grid; *Buizza et al.*, 1998), with T42L31 singular vectors.

◆ In 1998 initial uncertainties due to perturbations that had grown during the 48 hours previous to the starting time (evolved singular vectors, *Barkmeijer et al.*, 1999) were included, and a scheme to simulate model uncertainties due to random model error in the parametrized physical processes was introduced (*Buizza et al.*, 1999). EPS wave forecasts became available following the introduction of the coupled atmosphere-wave model in the forecast model (*Saetra & Bidlot*, 2002, *Janssen et al.*, 2005).

◆ In 2000, following the resolution increase of the ECMWF data-assimilation and high-resolution systems from T319L31 to T511L60, the EPS resolution was upgraded to T255L40 (*Buizza et al.*, 2003), with T42L40 singular vectors. The wave model resolution was increased to a grid spacing of the order of 110 km.

◆ In 2002 tropical perturbations were added to the system (*Barkmeijer et al.*, 2001).

◆ In 2004 the Gaussian sampling method for generating the EPS initial perturbations using singular vectors was implemented (*Ehrendorfer & Beck*, 2003).

◆ On 1 February 2006, following another resolution increase of the ECMWF data-assimilation and high-resolution systems to T799L90, the EPS resolution was further increased to T399L62 (see the article by *Untch et al.* in this Newsletter), with T42L62 singular vectors. The wave model spectral resolution was increased to 30 frequencies and 24 directions respectively without any change to its horizontal resolution.

The most recent change is the first of a three-phase upgrading process that will lead to the implementation of the ECMWF Variable Resolution Ensemble Prediction System (VAREPS). This is designed to increase the ensemble resolution in the early forecast range and to extend the forecast range covered by the ensemble system initially to 15 days and eventually to one month. The planned merger of the medium-range ensemble and the monthly operational system is going to be carried out in three phases.

◆ *Phase 1 (February 2006)*: resolution increase of the 10-day EPS from T255L40 to T399L62.

◆ *Phase 2 (planned for the second half of 2006)*: extension of the forecast range to 15 days using VAREPS, with T399L62 (day 0-10) and T255L62 (day 9-15).

◆ *Phase 3 (planned for 2007)*: weekly extension of VAREPS to one month, with a T255L62 atmospheric resolution and ocean coupling introduced at day 10 (the precise configuration of this final stage of VAREPS is still to be finalized).

Only the first two phases are discussed here: the phase-3 extension to one month will be discussed in a forthcoming article.

The rationale behind a variable resolution approach

VAREPS aims to provide better predictions of small-scale, severe-weather events in the early forecast range, and skilful large-scale guidance in the medium forecast range. The strategy used to achieve these goals is (a) to resolve small-scales up to the forecast time when they are predictable and their inclusion has a positive impact on the forecast accuracy, and (b) not to resolve them later in the forecast range when including them has a smaller, less detectable impact. This strategy leads to a more cost-efficient use of the computer resources, with most of them used in the early forecast range to resolve the small but still predicable scales. It is worth noting that a similar approach to ensemble prediction is not new, since it has been used at the National Centers for Environmental Prediction (NCEP, Washington) since inception of their ensemble prediction system (*Toth & Kalnay*, 1997).

The planned operational configuration

Technically, each VAREPS member will be generated by a two-leg forecast:

◆ *leg-1*: T399L62, from day 0 to day 10.

◆ *leg-2*: T255L62, from day 9 to day 15.

The horizontal resolution of the wave model stays unchanged (~110 km), however *leg-1* is now run with the same spectral resolution as the deterministic forecast (30 frequencies and 24 directions). The second leg reverts to 25 frequencies and 12 directions.

VAREPS will also include two other constant-resolution

forecasts for calibration/validation purposes: a 15-day T399L62 forecast and a 15-day T255L62 forecast (these two extra forecasts will be added to the VAREPS suite following users' requests; data from these will be accessible from MARS in *stream* = ENFO as *type* = CV, *number* = 1, 2).

Key VAREPS technical characteristics

Users should be aware of three key VAREPS technical characteristics.

◆ *Leg-2 initial conditions* – Each *leg-2* forecast starts from a *leg-1* day-9 forecast (see Figure 1), interpolated at the T255L62 resolution (in other words, the *leg-2* initial state is defined by a *leg-1* forecast instead of analysis fields for all the state-vector variables). The 24-hour overlap period has been introduced to reduce the impact on the fields that are more sensitive to the truncation from the high to the low resolution (e.g. convective and large scale precipitation). High-resolution wave spectra are smoothed out to the lower spectral resolution of the second leg.

◆ *Accumulated fields* – Accumulated fields are accumulated from the start of the *leg-1* forecast. In the *leg-2* forecast, to accumulate from the start of *leg-1* , once the *leg-2* forecast reaches the end of the overlap period (24-hour, i.e. day-10 if counted from the beginning of the *leg-1* forecast), the accumulated fields are overwritten by the *leg-1* 10-day forecast fields interpolated onto the T255 reduced Gaussian grid.

◆ *FDB and MARS streams ENFO and EFOV* – In the Field Data Base (FDB) and the Meteorological Archival and Retrieval System (MARS), *leg-1* forecasts from day 0 to day 10, and *leg-2* forecasts from day 10 to day 15 are written in the MARS stream ENFO (Ensemble Forecast stream), while *leg-2* forecasts from day 9 to day 10 are written in the new MARS stream EFOV (Ensemble Forecast Overalp stream). The *leg-1* 10-day forecast fields interpolated on the T255 reduced Gaussian grid are archived in the overlap stream, so that they can retrieved if needed (e.g. to correctly compute accumulated fields across the truncation forecast step). Similarly, ensemble wave fields are written in, respectively, streams WAEF and WEOV.

For a more detailed description of how to compute accumulated fields across the truncation forecast step (i.e. after forecast day 10), the reader is referred to the document "*Computation of accumulated fields in VAREPS*", accessible from the ECMWF web site at:

www.ecmwf.int/products/data/operational_system/evolution/ evolution_2006.html

These set-ups ensure that only users interested in using VAREPS forecast for accumulated fields after forecast day 10 need to take care when constructing fields accumulated between two forecast steps that include the truncation step.

Expected average impact of introducing VAREPS

To assess the impact of the introduction of VAREPS, ensembles run with an earlier VAREPS configuration with a day-7 truncation, a 13-day forecast length and 40 vertical levels have been compared with two constant-resolution ensemble configurations.
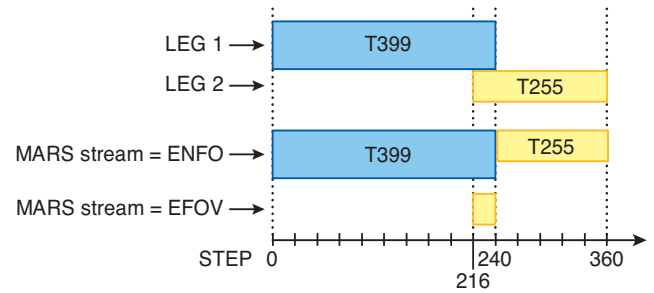
Figure 1 Schematic of the two-leg VAREPS planned for operational implementation, with MARS data streams ENFO and EFOV.

◆ *T255*: T255L40(day 0–13), with a 2700 second time step (this was the EPS configuration operational before 1 February 2006).
◆ *VAREPS*: T399L40(day 0–7) with a 1800 second time step and T255L40(day 6–13) with a 2700 second time step.
◆ *T319*: T319L40(day 0–13) with a 1800 second time step.

The second and the third configurations require ~3.5 times the computing requirements of the first configuration. Hereafter, the average performance of these configurations in providing probabilistic predictions of 500 hPa geopotential height, 850 hPa temperature and total precipitation anomalies over the Northern Hemisphere are compared. Apart from the resolution, these ensembles used the same model cycle, started from the same analysis, had the same set of initial perturbations and were based on 50 perturbed plus 1 unperturbed forecast.

Verification: T255(day 0–13) EPS versus VAREPS T399(day 0–7)+T255(day 7–13)

Figure 2 shows the 60-case average area under the relative operating characteristic curve and the Brier Skill Score for the probabilistic prediction of total precipitation in excess of 10 mm over 12 hours, for the T255 EPS and VAREPS. The forecasts are verified against a proxy of observed precipitation defined by the 24-hour forecast of the operational, high-resolution system. These 60 cases span a five-year period, and include both severe and non-severe event cases (in selecting these cases care was taken not to introduce any bias in the sample). This figure also shows the value of the rank-sum Mann-Whitney-Wilcoxon (RMW) significance test (computed using a bootstrapping technique): this test measures the probability that the distributions of scores for the systems may come from the same overall population. For example, RMW values of 10% indicate that there is a 10% chance that the distributions of the two scores coincide. Figure 2 shows that VAREPS has higher average scores than T255 up to forecast day 7 for the 10 mm/12 h threshold, with RMW values below 10% in the first case and 20% in the second one. Results also indicate that after the truncation step the difference between the two systems is not statistically significant.

Figure 3 shows the 60-case average area under the relative operating characteristic curve and the Brier Skill Score for the probabilistic prediction of positive 850 hPa temperature and 500 hPa geopotential height anomalies, for the T255
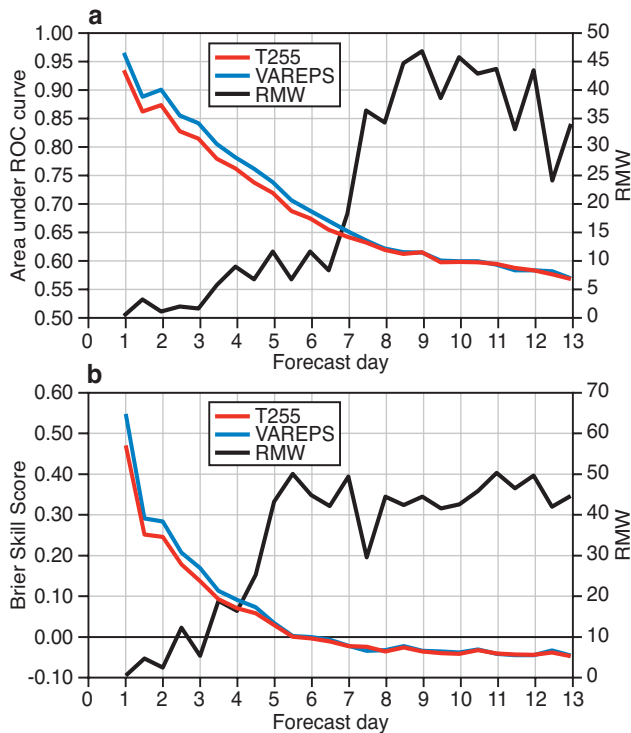
Figure 2 (a) 60-case average area under the relative operating characteristic (ROC) curve for the probabilistic prediction of total precipitation in excess of 10 mm/12 h over the Northern Hemisphere for T255 EPS (red line, left axis) and VAREPS (blue line, left axis), and the value of the rank-sum Mann-Whitney-Wilcoxon significance test (RMW, black line, right axis). (b) As (a) but for the Brier Skill Score, computed against climatology.

EPS and VAREPS, verified against the ECMWF analysis. Results indicate that the difference between these two systems in terms of the prediction of these two other variables still favours the VAREPS, but the RMW test has values below 20% only up to forecast day 5.

It is worth pointing out that the area under the relative operating characteristic for the prediction of both 850 hPa temperature and 500 hPa geopotential height stays above 0.7 for the whole forecast range. This suggests that VAREPS can provide valuable probabilistic forecasts beyond 10 days (note that the current operational EPS stops at day 10).

Equal-cost comparison: T319(day 0–13) versus T399(day 0–7)+T255(day 7–13)

An assessment has been made of the relative improvement (compared to the T255 EPS) of two ensemble configurations that require the same amount of computing resources to be completed: VAREPS and a contant-resolution T319 ensemble system. Figure 4 shows the percentage differences between average values (computed for 45 of the 60 cases shown in Figures 2 and 3) of the area under the relative operating characteristic for total precipitation in excess of 10 mm/12 h and positive 850 hPa temperature anomalies. Positive/negative relative differences mean that VAREPS/T319 outperforms/underperforms the T255 EPS.

Overall, results indicate first of all that both VAREPS and T319 outperform the T255 EPS, and, although the

difference between the VAREPS and the T319 performances is small, that VAREPS is associated with a larger relative improvement than T319.

Impact of increased resolution in the short-range for selected cases

The results discussed so far suggest that VAREPS is, on average, a better system than the T255 ensemble that was operational up to the end of January 2006. The average differences are small but statistically significant with a RMW value below 20% up to forecast day 7. Results indicate also that VAREPS is to be preferred to a constant-resolution, equal cost T319 ensemble. The average results have also indicated that the differences are more detectable in the early forecast range, and especially if one considers fields characterized by small-scale features such as total precipitation.

Two synoptic cases are now discussed to illustrate the positive impact of increasing the resolution in the early forecast range from T255 to T399 in severe weather events.

Hurricane Katrina (29 August 2005)

The first case is very recent: Hurricane Katrina, one of the strongest storms of the last 100 years. Katrina started to develop as a tropical depression on 23 August south-east of the Bahamas, reached category 5 on 28 August and category 4 when it landed on the 29th. At landfall, close to New
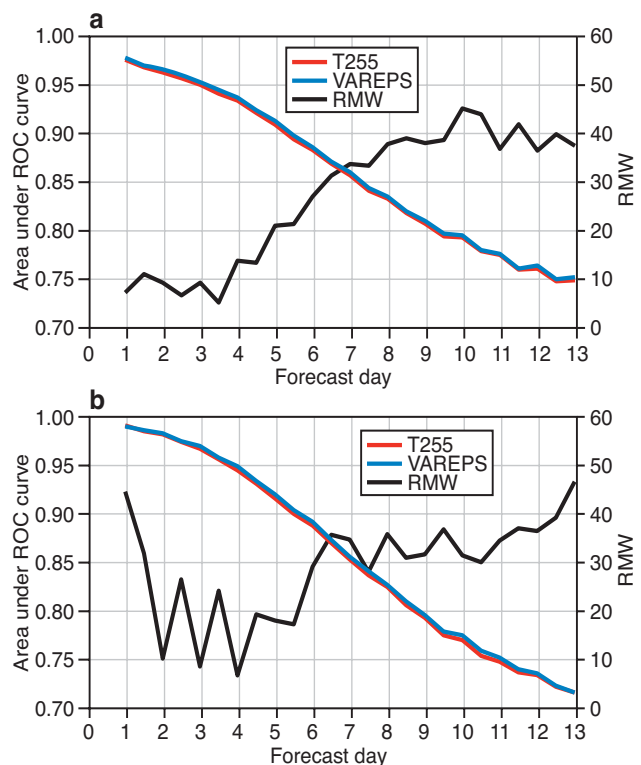
Figure 3 (a) 60-case average area under the relative operating characteristic (ROC) curve for the probabilistic prediction of positive 850 hPa temperature anomalies over the Northern Hemisphere for T255 EPS (red line, left axis) and VAREPS (blue line, left axis), and the value of the rank-sum Mann-Whitney-Wilcoxon significance test (RMW, black line, right axis). (b) As (a) but for the probabilistic prediction of positive 500 hPa geopotential height anomalies.

Orleans, sustained winds of more than 220 km/h were detected.

Figure 5 shows the intensity error (IE) and position error (D) of mean-sea-level-pressure (MSLP) minima predictions by the ensembles members of the T255 EPS, T319 system and VAREPS, with an 84, 72, 60 and 48 hour time lead. Ensemble forecasts have been clustered in three categories, accordingly to the intensity and position errors: (*IE*<5 hPa, *D*<100 km), (*IE*<15 hPa, *D*<200 km) and (*IE*<30 hPa, *D*<300 km), with the first category identifying forecasts with very small errors. Accordingly to this accuracy measure, the T399L40 VAREPS has the highest number for all forecast ranges and for all categories apart for the T+60 h forecast for the category (*IE*<5 hPa, *D*<100 km).

As a consequence of the more accurate development and intensification of the hurricane in each ensemble member, significant wave height (SWH) probabilistic forecasts for the Gulf of Mexico are more accurate in the T399L40 VAREPS. This can be seen, for example, by comparing the 84-hour probability forecasts of SWH in excess of 8 m (Figure 6). The T255 system gives no probability of SWH exceeding 8 m and the T319 system gives a 2–5% probability, while the T399L40 VAREPS gives a 10–20% probability correctly located in the area where SWH exceeded 8 m in the ECMWF operational analysis. Similar differences are detected by comparing probabilistic forecasts for earlier forecast ranges.

In the case of Katrina, the highest resolution T399L40 VAREPS rightly intensified the hurricane development, thus

improving probabilistic predictions of other surface variables such as wind speed and SWH. But it is worth mentioning that this is not because the T399L40 model systematically intensifies cyclonic developments. For example, in the case
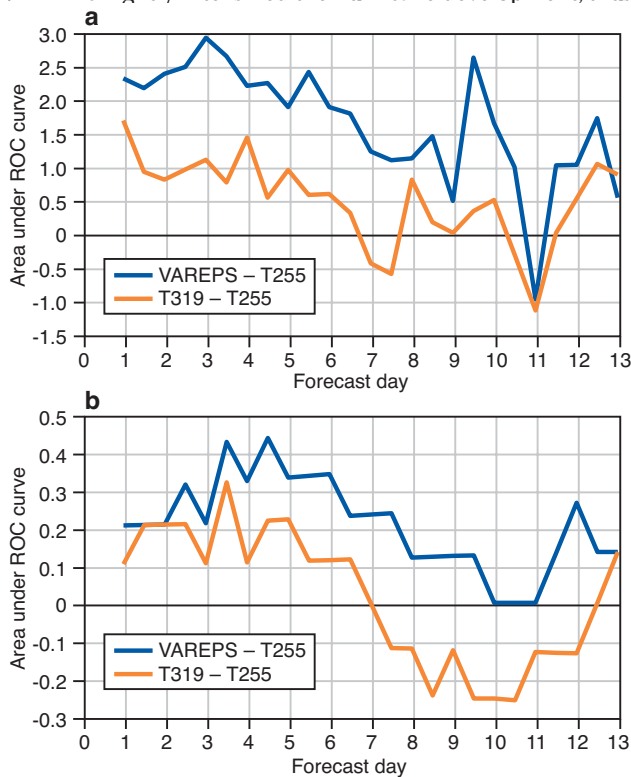
Figure 4 (a) Differences of 45-case average of the area under the relative operating characteristic (ROC) curve for the probabilistic prediction of total precipitation in excess of 10 mm/12 h over the Northern Hemisphere between VAREPS and T255 EPS (blue line) and between T319 system and T255 EPS (yellow line). (b) As (a) but for the probabilistic prediction of positive 850 hPa anomalies.
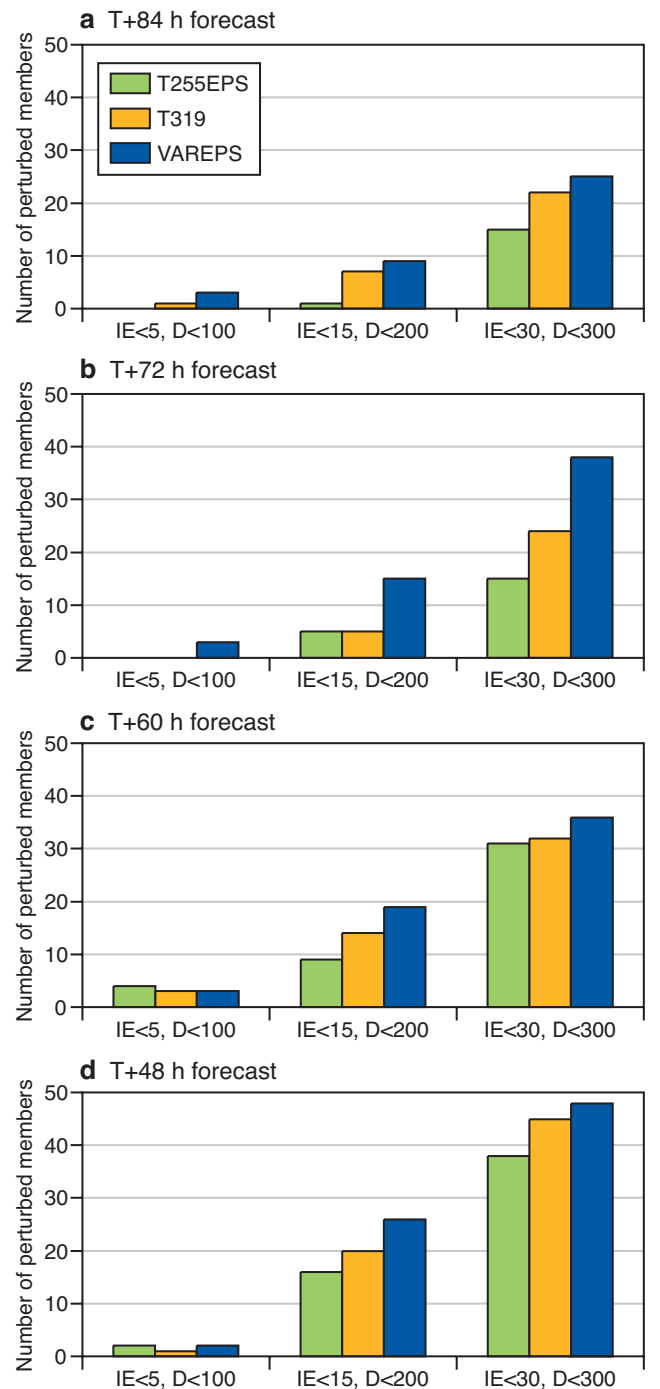
Figure 5 Mean-sea-level-pressure (MSLP) intensity and position error statistics for Hurricane Katrina for the T255L40 operational EPS, T319L40 system and T399L40 VAREPS forecasts valid for 12 UTC on 29 August 2005 using (a) T+84 hour, (b) T+72 hour, (c) T+60 hour and (d) T+48 hour forecasts. "IE < X, D < Y" refers to forecasts with intensity error less than X hPa and position error less than Y km (e.g. IE < 5, D < 100 indicates is the number of forecasts with intensity error less than 5 hPa and position error less than 100 km. Forecasts have all been verified against the operational TL511L60 analysis.

of Hurricane Stan, a system that caused severe damage and loss of life in Guatemala because of a land-slide induced by the intense precipitation, the T399L40 VAREPS forecasts outperformed the T255L40 and T319L40 forecasts mostly by positioning more accurately the area affected by the intense precipitation, rather than in the intensification of the cyclone.

Firenze flood (4 November 1966): The famous 'Alluvione di Firenze'

The second case is an historical one, the flood of North-Eastern and Central Italy of November 1966. This flood event is known as "l'alluvione di Firenze del '66", since Firenze was the most famous Italian city affected by it. As one of the most severe over Europe, this flood caused severe damage to the historical towns of Florence and Venice, disruption in the Po' Valley and in Tuscany, including loss of lives.

Figure 7 shows the T+48 to T+72 hour probabilistic prediction of total precipitation in excess of 75 and 150 mm given by the T255 EPS (Figures 7(a) and 7(c)) and the T399 VAREPS (Figures 7(b) and 7(d)) valid for the 24-hour period starting at 12 UTC on 3 November. These probability maps can be compared with the proxy for precipitation verification given by a T511L60 forecast started at 12 UTC on 3 November (Figure 7(e)). It is worth mentioning that this proxy

field represents rather accurately the overall pattern of the observed precipitation field, but underestimates the maximum values (during the verification period, maximum values of between 200 and 400 mm were observed in Tuscany, and between 300 and 700 mm in North-Eastern Italy.

Figure 7 shows that higher probability values are predicted by the T399 VAREPS both over Tuscany and North-Eastern Italy in the areas where intense precipitation was detected. It is interesting to point out that the T399 VAREPS gives also a 40-60% probability that precipitation could exceed 150 mm over North-Eastern Italy, correctly indicating that this area was going to be affected by the most intense rainfall.

Planned implementation schedule

The implementation on 1 February 2006 of the T399L62 (day 0-10) ensemble prediction system completed the first of a three-phase upgrading process that will lead to the implementation of the ECMWF Variable Resolution Ensemble Prediction System (VAREPS). This is designed to increase the ensemble resolution in the early forecast range and to extend the forecast range covered by the ensemble system initially to 15 days and eventually to 32 days, following the planned merger of the medium-range and the monthly ensemble forecasting systems.
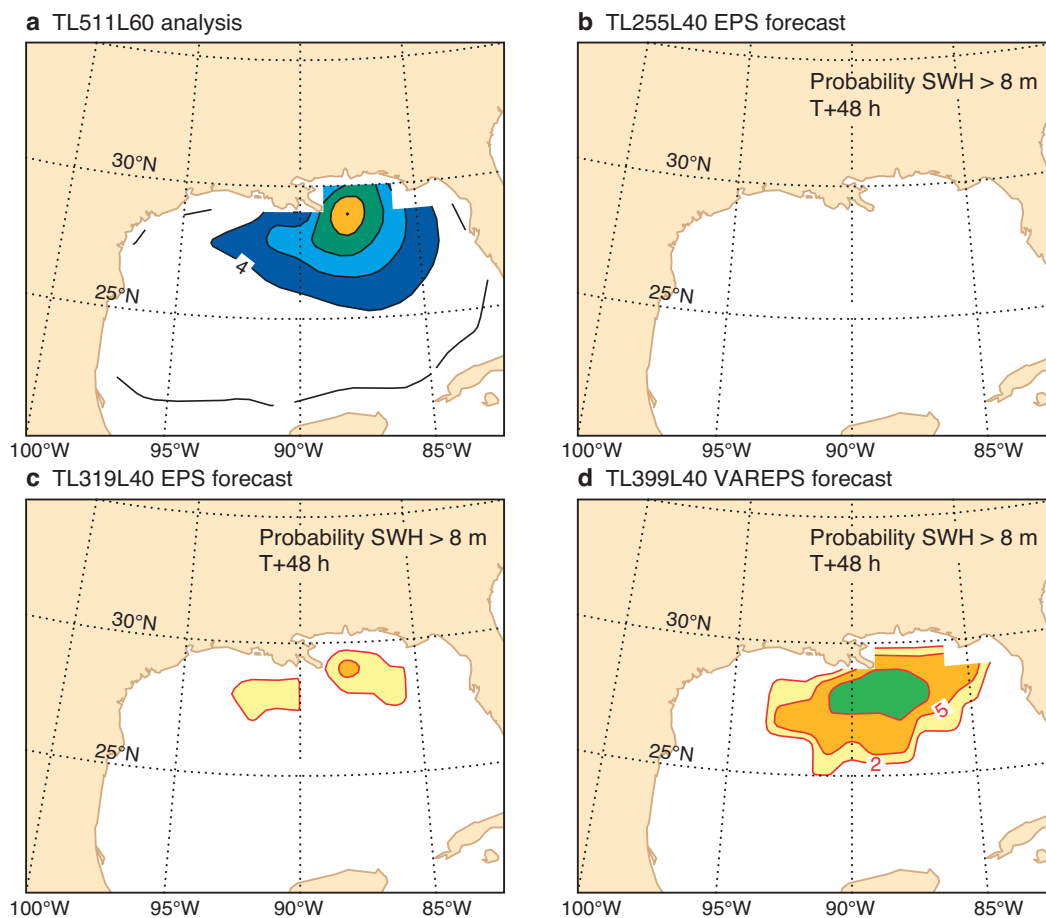
Figure 6 Forecasts of significant wave height (SWH) for Hurricane Katrina. (a) SWH from the operational T511L60 analysis valid at 12 UTC on 29 August 2005 (contour interval 2 m). (b) T+84 hour forecast of the probability of SWH higher than 8 m from the T255L40 operational EPS. (c) As (b) but from the T319L40 EPS. (d) As (b) but from the T399L40 VAREPS. Contour isolines for probabilities are 2, 5 and 10%.

a TL255L40 EPS forecast

Probability TP > 75 mm / 24 h
T+48 h to T+72 h

b TL399L40 VAREPS forecast

Probability TP > 75 mm / 24 h
T+48 h to T+72 h

c TL255L40 EPS forecast

Probability TP > 150 mm / 24 h
T+48 h to T+72 h

d TL399L40 VAREPS forecast

Probability TP > 150 mm / 24 h
T+48 h to T+72 h

e Verification proxy
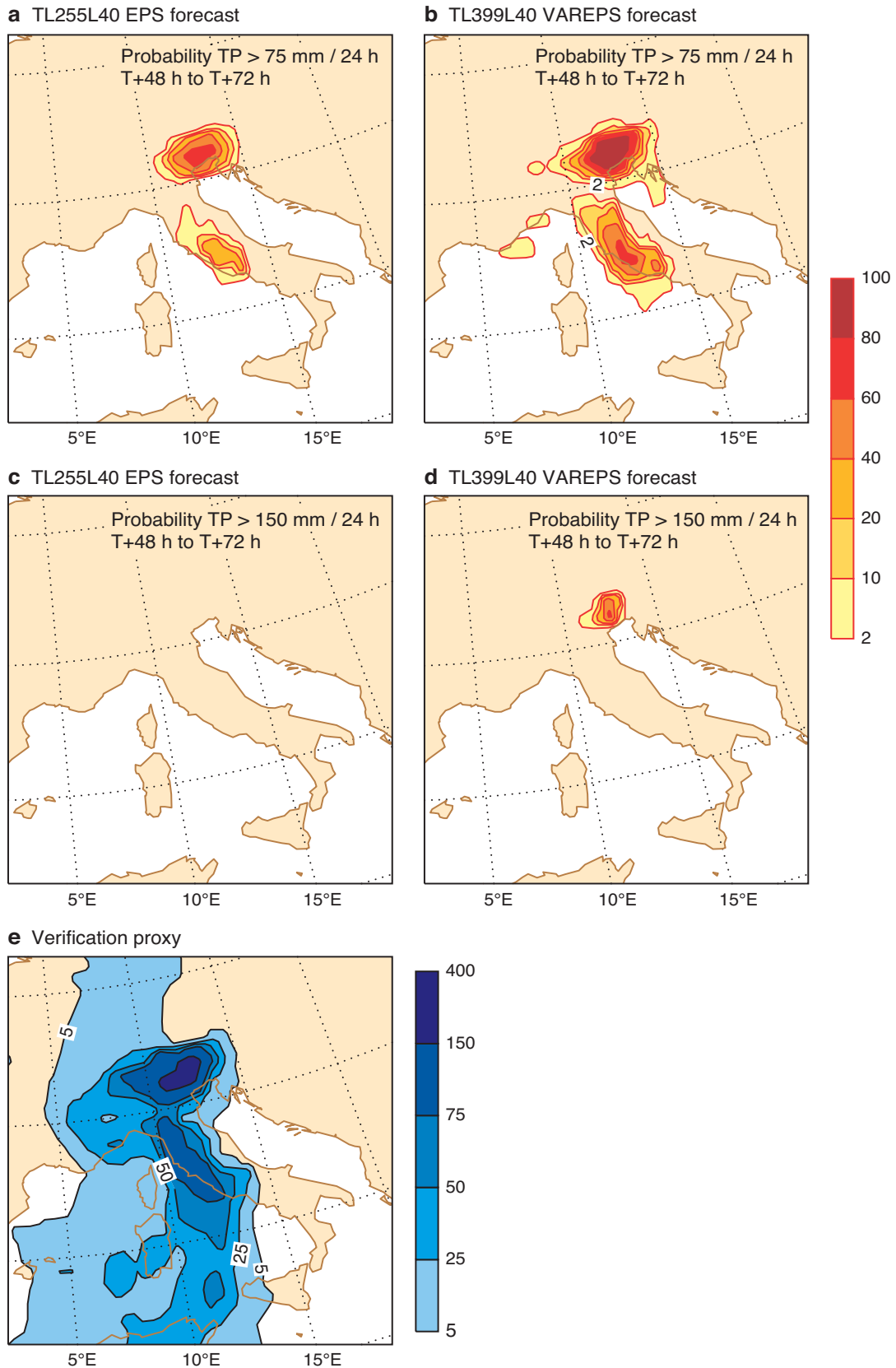
Figure 7 Probabilistic predictions of 24-hour total precipitation (TP) for the 1966 Italian flood. Forecasts started at 12 UTC on 1 November 1966 and are valid for the 24-hour period starting at 12 UTC on 3 November. (a) T + 48 to T + 72 hour EPS prediction of the probability of TP in excess of 75 mm/24 h. (b) As (a) but for T399 VAREPS. (c) T + 48 to T + 72 hour EPS prediction of the probability of TP in excess of 150 mm/24 h. (d) As (c) but for T399 VAREPS. (e) Verification proxy given by the T + 24 hour T511L60 prediction of TP started at 12 UTC on 3 November. Contour isolines for probabilities are 2, 10, 20, 4, 60 and 80%, and for TP 5, 25, 50, 75, 150 and 400 mm.

The second of this three-phase process, planned for the second half of 2006, will lead to the extension of the 00 and 12 UTC ensemble systems to 15 days using the VAREPS approach, with a T399L62 resolution up to forecast day 10 and a T255L62 resolution between forecast day 10 and 15.

VAREPS will further increase the value of the ECMWF probabilistic forecasting system, and deliver to ECMWF users more accurate predictions of small-scale, severe weather events in the early forecast range and skilful probabilistic predictions of larger scale features in the medium forecast range.

FURTHER READING

Barkmeijer, **J.**, **R. Buizza** & **T.N. Palmer**, 1999: 3D-Var Hessian singular vectors and their potential use in the ECMWF Ensemble Prediction System. *Q. J. R. Meteorol. Soc.*, **125**, 2333–2351.

Barkmeijer, **J.**, **R. Buizza**, **T.N. Palmer**, **K. Puri** & **J.-F. Mahfouf**, 2001: Tropical singular vectors computed with linearized diabatic physics. *Q. J. R. Meteorol. Soc.*, **127**, 685–708 (also available as *ECMWF Technical Memo. No. 297*).

Buizza, **R.** & **T.N. Palmer**, 1995: The singular-vector structure of the atmospheric global circulation. *J. Atmos. Sci.*, **52**, 1434–1456 (also available as *ECMWF Technical Memo. No. 208*).

Buizza, **R.**, **T. Petroliagis**, **T.N. Palmer**, **J. Barkmeijer**, **M. Hamrud**, **A. Hollingsworth**, **A. Simmons** & **N. Wedi**, 1998: Impact of model resolution and ensemble size on the performance of an ensemble prediction system. *Q. J. R. Meteorol. Soc.*, **124**, 1935–1960 (also available as *ECMWF Technical Memo. No. 245*).

Buizza, **R.**, **M. Miller** & **T.N. Palmer**, 1999: Stochastic representation of model uncertainties in the ECMWF ensemble prediction system. *Q. J. R. Meteorol. Soc.*, **125**, 2887-2908 (also available as *ECMWF Technical Memo. No. 279*).

Buizza, **R.**, **D.S. Richardson** & **T.N. Palmer**, 2003: Benefits of increased resolution in the ECMWF ensemble system and comparison with poor-man's ensembles. *Q. J. R. Meteorol. Soc.*, **129**, 1269-1288 (also available as *ECMWF Technical Memo. No. 389*).

Ehrendorfer, **M.** & **A. Beck**, 2003: Singular vector-based multivariate sampling in ensemble prediction. *ECMWF Technical Memo. No. 416*.

Janssen P., **J.-R Bidlot**, **S. Abdalla** & **H. Hersbach**, 2005: Progress in ocean wave forecasting at ECMWF. *ECMWF Technical Memo. No. 478*.

Molteni, **F.**, **R. Buizza**, **T.N. Palmer** & **T. Petroliagis**, 1996: The ECMWF ensemble prediction system: methodology and validation. *Q. J. R. Meteorol. Soc.*, **122**, 73–119 (also available as *ECMWF Technical Memo. No. 202*).

Saetra, **Ø.** & **J.-R Bidlot**, 2002: Probabilistic forecasts of ocean waves. *ECMWF Newsletter No. 95*, 2–9.

Toth, **Z.**, & **Kalnay**, **E.**, 1997: Ensemble Forecastign at NCEP and the breeding method. *Mon. Wea. Rev.*, **125**, 3297–3319.

Untch, **A.**, **M. Miller**, **M. Hortal**, **R. Buizza**, & **P. Janssen**, 2006: Towards a global meso-scale model: The high-resolution system TL799L91 and TL399L62 EPS. *ECMWF Newsletter No. 108*, 6–13.

Surface pressure bias correction in data assimilation

Drasko Vasiljevic, Erik Andersson, Lars Isaksen, Anotonio Garcia-Mendez

I t is well known that the surface pressure (Ps) observations reported by a large number of SYNOP land and sea (SHIP) stations as well as drifting buoy (DRIBU) stations are biased, and in many cases by several hPa. These biases are mostly related to incorrect assumptions about the station heights, and remain fairly constant in time. Therefore, several hundred stations would normally appear on the ECMWF blacklist due to a significant long-term bias.

A new scheme for estimating and correcting Ps bias, based on an adaptive correction method, was introduced into the ECMWF operational analysis/forecasting system on 5 April 2005. The scheme has had a positive impact on both the analysis and forecast, and has reduced the number of stations on the blacklist.

Bias correction method

A few years ago Peter Janssen proposed an adaptive method for bias correction of Ps time series. The method is based on linear estimation theory and is referred to as the OI method. This provides estimates of the bias and its confidence, station by station, based on a time series of observation-minus-background departures. Furthermore, the method relies on two assumptions: (a) the observational Ps bias is local for a given station (i.e. no spatial correlation) and (b) there is no, or only small, model bias. For more details see the Appendix.

Experiments have been carried out to examine the behaviour of the OI method. Figure 1 shows Ps departures and the bias correction time series using the OI bias estimates. This is for SYNOP station 65355 (Niamtougou, Togo) for February–April 2005. It can be seen that the station has a bias of about -11 hPa. The OI method clearly identified the bias and appears to be a smooth operator.

Practical aspects

A central component of the bias correction scheme is its database, PSBIAS. The PSBIAS is a hierarchical database modelled on ECMWF's operational ODB (Observation Data Base) and it plays a key role in providing the cycling mechanism for the Ps bias correction scheme. The PSBIAS is structured in such a way that the database main entry points are stations. Each station, or entry point, is further divided into two parts: (a) header and (b) body, which are appropriately linked. All relevant bias correction parameters needed to be carried forward in time to perform the bias correction are kept in the header, whereas the body part keeps the station time record. The time record is up to one month long for hourly observations and longer for less frequent observations.
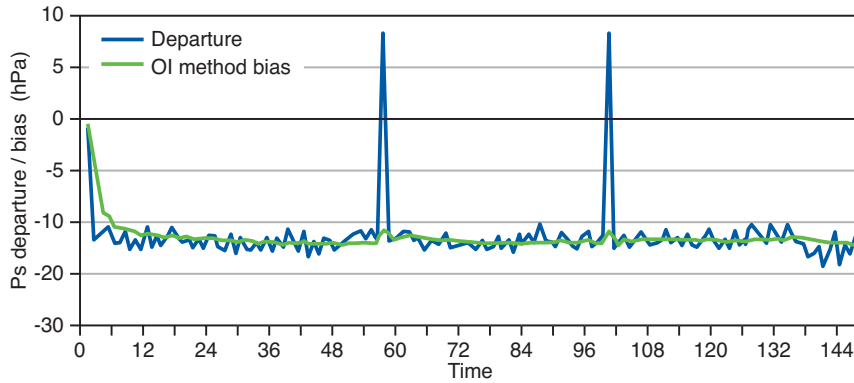
Figure 1 Ps departure/bias time series (February–April 2005) for SYNOP station 65355: Ps departure (blue) and OI method bias estimate (green).

Not all Ps observing stations are considered for bias correction. For example, stations for which either station altitude is missing or the height difference between station and model is more than 200 m are omitted. Furthermore, a Ps observation is discarded if the observation departure is bigger than 15 hPa or reported pressure is mean-sea level pressure but the station is above 500 m. Bias estimates are calculated only if the station sample size is big enough. At the moment the sample size limit is set to 30. Once this number is reached the station is assumed to be purely biased only if its bias estimate is bigger than one standard deviation. Additionally, in order to avoid correcting for possible small model biases, any bias estimates less then 1 hPa are not considered. Also, bias estimates which are too old are not used. Currently, bias estimates older than 5 days are considered to be old. In that case they are recalculated from scratch (cold start), once a sufficient new sample is available.

As an illustration of the impact of the bias correction scheme, Figure 2 shows the bias corrected Ps departure (red) along with the original Ps departure (blue) and applied Ps bias correction (green) for the same SYNOP station as used in Figure 1. To start with there is no bias correction because the sample size is not big enough (the warm up period). Once the bias correction kicked in, it was correcting departures quite nicely. It can also be seen that at the beginning the scheme was turning itself on and off a few times before settling in. This station's stable long-term bias was interrupted a couple of times during this period. This was a result of two out of sequence departures. Obviously in these two cases the bias correction scheme made it even worse but recovered quickly. As it turned out, this station is RDB (Report Data Base) flagged because of its wrong alti-

tude; hence it was not used even after bias correction. However, by closer examination of the first guess check flags in both the "*no Ps bias correction*" and the "*Ps bias correction*" runs, it was found out that in the "*no Ps bias correction*" run the Ps was flagged and rejected, whereas in the "*Ps bias correction*" run the Ps was not flagged and would have been used in the analysis if it was not for the overriding RDB station height flag. It would be quite possible to come up with a practical scheme whereby biased stations, like this one, could have their altitude "corrected" by using the long-term bias. Likewise, a similar mechanism could be applied for blacklisted biased stations. Blacklisted stations have been monitored after bias correction was introduced and many stations have been taken off the blacklist.

Figure 3 shows another example of a Ps biased station (SYNOP 82353, Altamira, Brazil). However, in this case the station height is thought to be correct and the real reason for being biased was not known. Again, after the warm up period, the bias correction scheme turned itself on and was correcting the Ps by about -3 hPa. After closer examination of this station it was found that in the "*no Ps bias correction*" run Ps was surviving (just) the first guess check but only to be rejected by the analysis check. On the other hand in the "*Ps bias correction*" run it passed all the checks and it was used in the analysis. However, there were two occasions when it failed the first guess check. It first happened when the original Ps departure became positive (in a long sequence of negative ones) and after bias correction it became even bigger. The second time the original departure happened to be about twice its usual negative size. The bias correction scheme did correct it, but the departure was still too big – hence it was rejected.
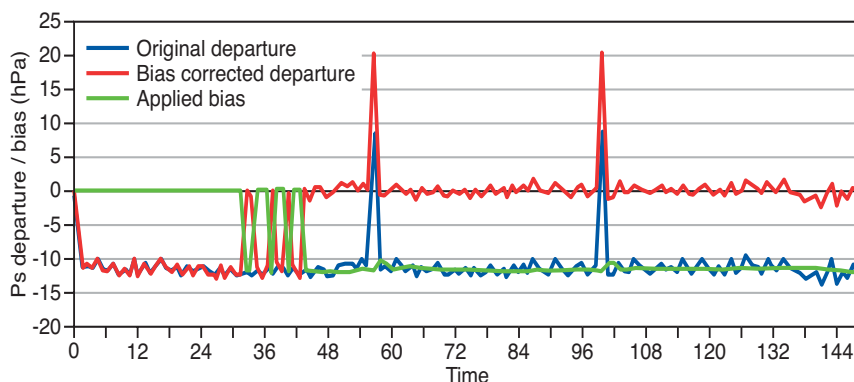
Figure 2 Ps departure/bias time series (February-April 2005) for SYNOP station 65355: original Ps departure (blue), bias corrected Ps departure (red) and applied Ps bias (green).

21
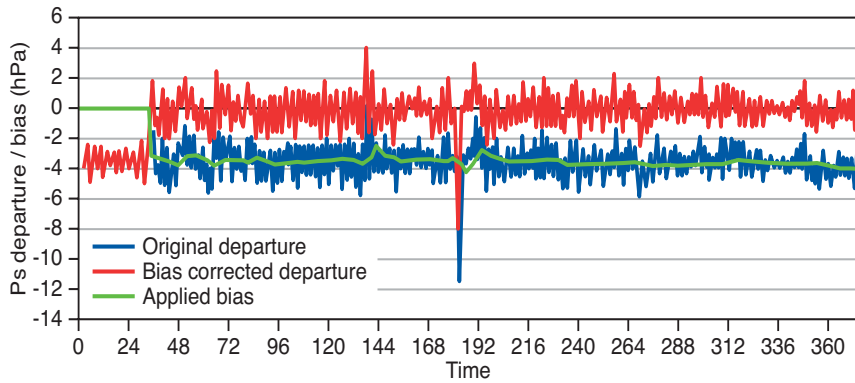
Figure 3 Ps departure/bias time series (December 2004–April 2005) for SYNOP station 82353: original Ps departure (blue), bias corrected Ps departure (red) and applied Ps bias (green).

Analysis and forecast impacts

Experiments with the Ps bias correction scheme

Prior to the operational implementation of the Ps bias correction scheme a number of experiments with and without Ps bias correction have been performed. They have all shown the expected results. In these experiments there were several hundred bias corrected stations. Analysis increments were somewhat smaller and the impact on forecast scores was about neutral. Eventually, E-suite or E-suite type experiments were carried out (the E-suite is used to test possible operational changes).

There was a long E-suite type experiment with Ps bias correction switched on from 1 August 2004 till 31 December 2004. Furthermore, the E-suite was then run from the 1 January 2005 till the operational implementation on 5 April 2005. Additionally, just for August there was another E-suite type experiment without the Ps bias correction shadowing the above mentioned E-suite type experiment. Comparing these two August E-suite type experiments there were no surprises coming from the Ps bias correction. At the end of the month about 800–1000 biased stations were identified and the correction scheme itself seemed to have

performed satisfactorily. Overall there was a better fit to Ps observations with average analysis increments slightly reduced. The impact on the forecast in terms of geopotential anomaly correlation scores for 10-day forecasts was neutral for the northern hemisphere and slightly positive in the southern hemisphere.

The E-suite type experiment with Ps bias correction went on till the end of December 2004. Unfortunately, the forecast scores did not look that good in December. In the southern hemisphere the impact was still about neutral, but rather negative in the northern hemisphere. Negative results were obtained also for North Pacific, North America, North Atlantic and Europe. It is for that reason that a new E-suite type experiment for December with the Ps bias correction turned off was carried out. This new experiment was started from the already running E-suite type experiment. The mean-sea level pressure analysis differences between these two experiments for the very first analysis cycle are shown in Figure 4.

As it can be seen in Figure 4, most differences are small and local as expected. However, there is a rather large-scale positive difference over the North America (Canada/ USA). This was not expected and merited further investigation.
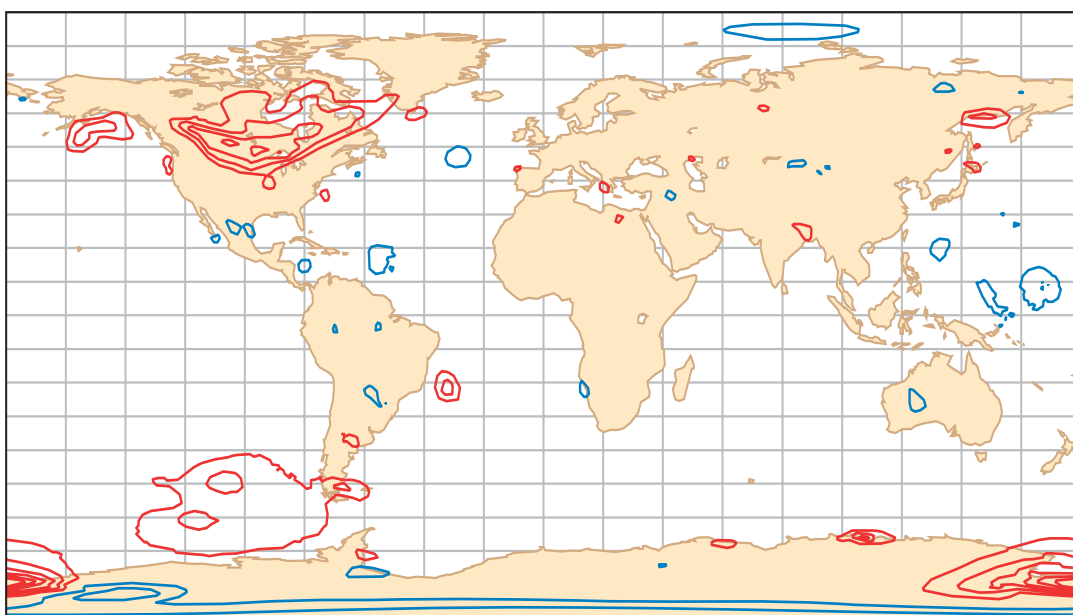
Figure 4 PMSL analysis difference ("*Ps bias correction*" minus "*no Ps bias correction*") for 00 UTC on 1 December 2004: positive (red) and negative (blue); 0.5 hPa contouring interval.

Investigation of the large difference between experiments over North America

Looking at the daily PMSL analysis difference between the two experiments, it was found that the "*BLOB*" stayed over North America for about two weeks, though it did move around slightly. Furthermore, the "*BLOB*" survived in the ensuing forecasts and propagated downstream with the flow contributing to the bad forecast scores. There was no immediate answer to what went wrong.

The first thing which came to mind was that the Ps bias correction scheme somehow went wrong. Checking the PSBIAS database it was found out that for this particular analysis cycle about 80 stations in the area were bias corrected. These 80 stations accounted for about 600 out of 1,000 reports for the 12-hour data window. Out of these 600 reports about 200 were SYNOP and 400 were METAR reports. The size of the Ps bias ranged from -1 hPa to -3 hPa. Thus, all stations were negatively biased. The large-scale pattern was not expected as our first assumption when designing the Ps bias correction scheme was that observational Ps bias is not spatially correlated. Looking at the bias time series for these stations leading to the analysis cycle in question one could not see anything unusual in the scheme's behaviour.

Figure 5 shows the background and analysis fit to SYNOP Ps observations in the region. The black line represents the fit to data for the "*Ps bias correction*" run, whereas the red line represents the fit for the "*no Ps bias correction*" run. From the "*no Ps bias correction*" run it is clear that there was a bias of about -2 hPa. Furthermore, Figure 5 shows that in the case of the "*Ps bias correction*" run the scheme did a rather good job by, to a large extent, removing the bias. What Figure 5 also shows is that both analyses were a close fit to the observations. However, the analysis resulting from the "*Ps bias*

correction" run creates the "*BLOB*" which subsequently impacts (negatively) the forecast quality. At this point it became clear that further investigation was needed.

First of all, none of the just described behaviour was noticed during the August runs, thus raising the question what happened with Ps biases from September till December. In order to try to answer this question Ps departure time series for the Canada/USA region were looked at. The time series are shown for the E-suite type experiment with Ps bias correction (Figure 6(a)) and the operational version (Figure 6(b)) for SYNOP data from August till December 2004. Both time series clearly show that from August till late September there was not much bias in the Canada/USA region to start with. However, as from late September, bias started creeping in and growing. As discussed earlier, the bias correction scheme was recognising and correcting it. Since there was no bias correction in the operational system at the time the size of the bias was somewhat bigger.

Now it started looking as we might be dealing with a possible model bias. If true, the bias correction scheme should not be applied. This is because it would go against the second bias correction scheme assumption that there is no, or small, model bias. As mentioned earlier, in anticipation of something like this, although on a smaller scale, the 1 hPa limit on when to apply the bias correction had been introduced in an attempt to avoid correcting for possible small model biases. Also, what came as a surprise here was that there was no other region like Canada/USA where a similar problem could be found.

In order to facilitate understanding this problem further, a time series of maximum, minimum and average PMSL analysis differences for various scenarios and regions were looked at. What one expects to see from this type of time series is that both maximum and minimum differences vary
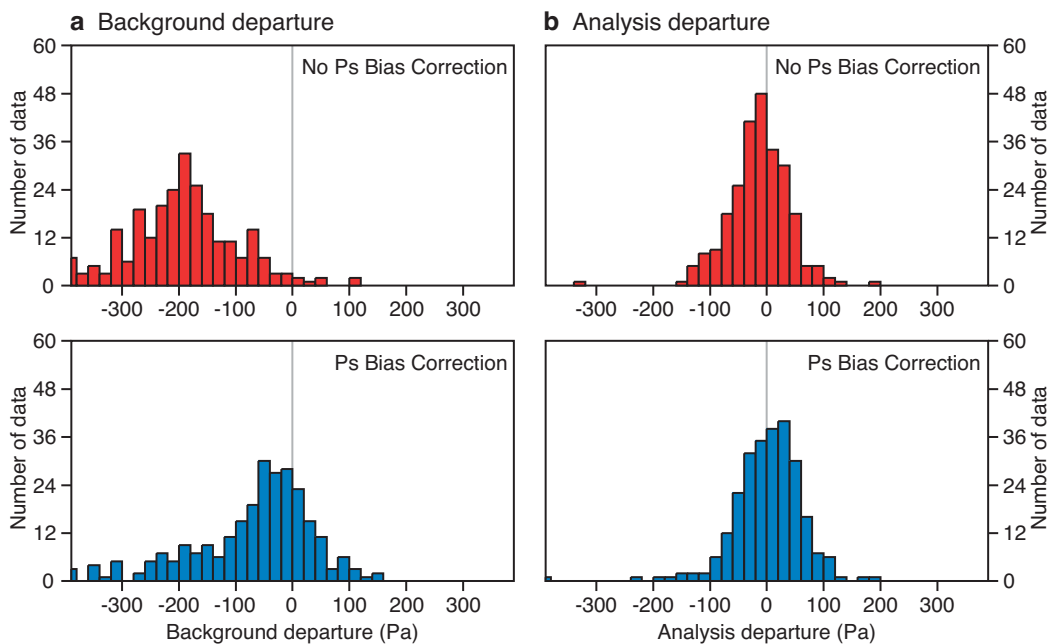
Figure 5 Background and analysis fit to SYNOP Ps data for 00 UTC on 1 December 2004 for Canada/USA: (a) background departure and (b) analysis departure; "no Ps bias correction" (red) and "Ps bias correction" (blue); units Pa.
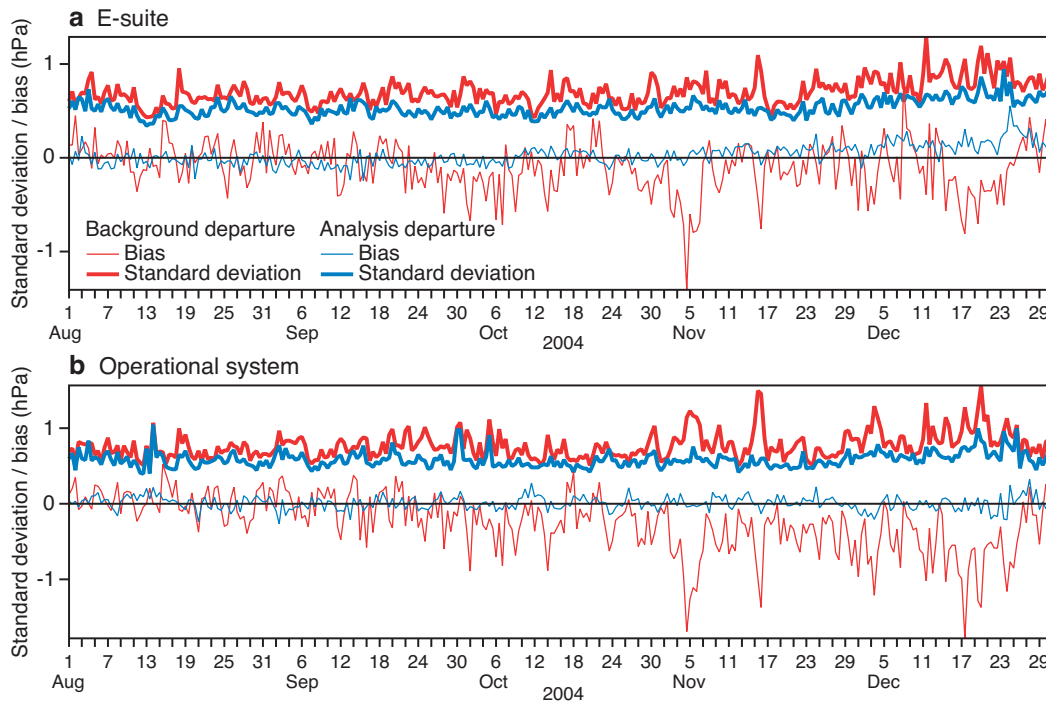
Figure 6 SYNOP Ps time series for 00 UTC on 1 August to 12 UTC on 31 December 2004 for Canada/USA for (a) E-suite and (b) operational system. Bias of background departures (thin red) and analysis departures (thin blue) with corresponding standard deviations in thick red and thick blue; units hPa.

day by day, whereas the average differences are stable and around 0 hPa. Time series of PMSL analysis differences between an E-suite type experiment with Ps bias correction and operational system for August–December period for the northern hemisphere are shown in Figure 7(a). Red and blue lines are maximum and minimum differences, respectively, and the black line is the average difference. As expected the maximum and minimum differences vary day by day, and the average difference stays rather stable and just hovers around 0 hPa.

Figure 7(b) shows differences for the Canada/USA region, and here we have a surprise. From August till late September the average differences are not as stable as previously seen with amplitudes of about 1 hPa, but still reasonable. However, from late September till the end of December the average differences are far from stable and are as big as 2 hPa, or even bigger. This result seems to coincide with the large-scale Ps bias noticed earlier. Unfortunately, we did not have the "*no Ps bias correction*" experiment for the whole of August–December. But there was one during December which was mentioned earlier. The average PMSL differences for "no Ps bias correction" run (not shown) are not that stable in the December either, though the amplitudes are not as big as in the in the "*Ps bias correction*" run, just going over 1 hPa.

Meanwhile, as the E-suite (started on 1 January 2005) was going on, the forecast scores improved and the December problem in the Canada/USA region was less and less evident.

All this was suggesting that we are dealing with unexpected model bias. The bias correction scheme presented and introduced here is only supposed to deal with uncorrelated observational Ps bias. Thus in the presence of a larger-scale model bias the correction should not be applied.

The following section will deal with possible ways of identifying and dealing with model bias.

Model versus observational bias

As just discussed correcting model bias by correcting observations leads to a rather poor result and it should not be done. The difficulty is how to identify the model bias and subsequently separate it from the observational one. It is worth remembering that we introduced a 1 hPa limit on when to apply the bias correction in order to avoid correcting for small model bias. Of course that limit could be increased to say 2 hPa. This rather quick fix should hopefully eliminate the problem which occurred over North America. However, since the limit is applied globally, the increase would unjustly exclude a number of genuinely biased stations from being corrected, therefore killing positive effects of the bias correction scheme. Thus a more selective solution to this problem should be sought.

The analysis of the problem presented in the previous section clearly indicated that when it happens a large number of stations are in agreement in terms of both the bias sign and the bias size. Now, remember that in the old ECMWF OI analysis system we used to have a quality control procedure called the "buddy" check which is not used in the current ECMWF analysis system. In brief, the idea was that in order to quality control a given observation one could actually do the analysis at that point without the observation itself being used. Then if analysed and observed values at that point agree within some limits one assumes that the observation is probably correct. Now if we turn this idea around, and if for a given biased station its bias value agrees, within limits, with the analysed bias from its neighbours with-
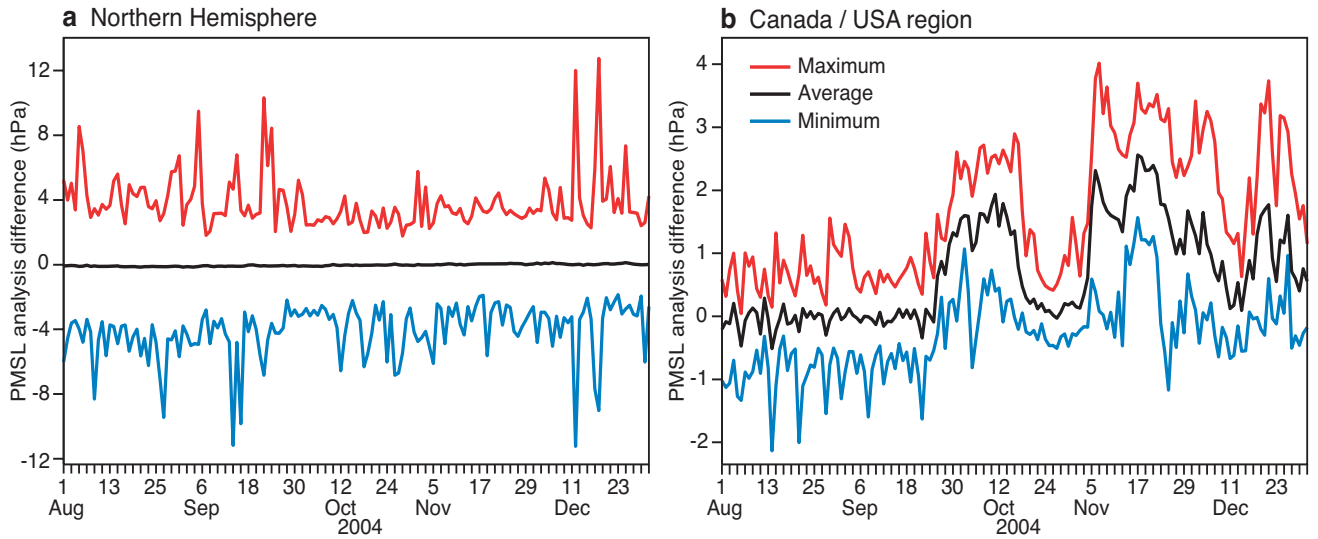
Figure 7 Maximum (red), minimum (blue) and average (black) PMSL analysis difference ("*Ps bias correction*" minus "*operational system*") for 00 UTC on 1 August to 00 UTC on 31 December 2004 for (a) the northern hemisphere and (b) Canada/USA region; units hPa.

out using the station itself, then one should not apply bias correction at that station. The neighbouring stations to be considered should be within a circle of a certain radius. Also, as an agreement limit, we could use for example the analysed bias value plus or minus a multiple of the standard deviation. But do not forget that there should be a limit on how many stations ought to be found in the vicinity. Since this type of check is very similar to the original "*buddy*" check but in the opposite sense, naming it the "*anti-buddy*" check sounded appropriate. Furthermore, there were at least two possibilities on how to perform the bias analysis from the neighbouring stations.

◆ One could do a simple statistical analysis, calculate the mean and standard deviation and use the mean as analysed bias value along with the standard deviation to perform the "*anti-buddy*" check.

◆ Instead of using the mean as the analysed bias value a type of two-dimensional univariate bias analysis could be performed.

The "*anti-buddy*" check has been added to the Ps bias correction scheme. First, as in the original scheme, a list of potentially biased stations is compiled and then for each of them the "*anti-buddy*" check is applied. The circle radius around a given station is set to 300 km. The number of influencing stations used to perform the "*anti-buddy*" check is set to 10 or more. The analysed bias value is assumed to be the mean bias and the agreement limit is set to an analysed bias value of ±2.0 standard deviations. Stations which do not have enough neighbours are not subjected to this check.

Figure 8 shows the PMSL analysis difference between what we now call the "*Ps bias correction plus anti-buddy check*" run and the original "*Ps bias correction*" run. As can be seen, the
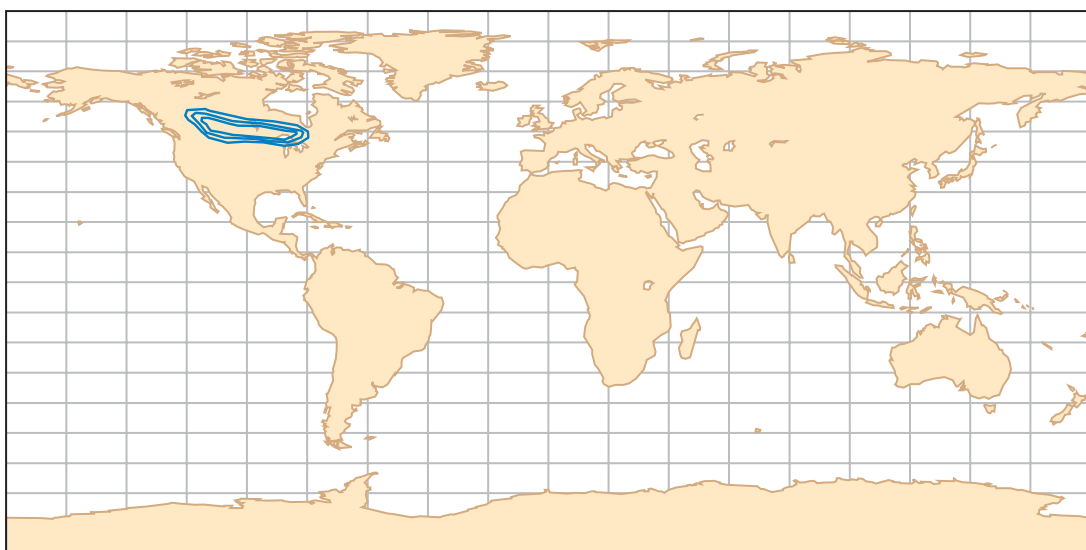
Figure 8 PMSL analysis difference ("*Ps bias correction plus anti-buddy check*" minus original "*Ps bias correction*") for 00 UTC on 1 December 2004: positive (red) and negative (blue); 0.5 hPa contouring interval.

map is mainly void except for the Canada/USA region where we experienced the problem before. This was a very good result. The "*anti-buddy*" check clearly had an impact only in the problematic region, and both the sign and the size of difference are good.

Now comes the all important question: if we were to rerun the E-suite type experiment with the "*anti-buddy*" check included for December, would that improve the forecast scores?

As mentioned earlier the original "*Ps bias correction*" run underperformed the "*no Ps bias correction*" experiment particularly in the northern hemisphere. The extent of the under performance in the northern hemisphere was also evident in the regional scores. The "*Ps bias correction plus anti-buddy check*" experiment has done a lot better in the northern hemisphere than the original "*Ps bias correction*" experiment. In the southern hemisphere, where there was not much of the problem anyway, there was little difference between the experiments. The improvement in the northern hemisphere scores was also found in the regional scores.

The "*anti-buddy*" check had a positive impact on both the analysis and forecast. Consequently it was included in the operational implementation of the Ps bias correction scheme.

To sum up

The Ps bias correction scheme based on the OI method for estimating and correcting Ps bias is now a part of the ECMWF operational system. The scheme identifies about 1,000 biased stations out of about 11,000 surface stations. The biases are mostly related to incorrect station height and remain more or less constant in time. The scheme is based on two assumptions: (a) Ps bias is local (no spatial correlation) and (b) no model bias, or very small model bias. When both of these assumptions are satisfied the scheme had a positive impact on both the analysis and forecast. However, in the presence of a larger model bias (both spatially and size wise) the scheme was not performing as well. Thus, an adjustment to the scheme was needed to recognise a possible model bias and separate it for the observational bias. The proposed "*anti-buddy*" check has managed to fulfil this requirement.

The Ps bias correction scheme has now been used operational for more than a year and has been performing well. Also, the scheme is being used in the re-analysis experiments and from the first runs it appears to be doing well there too.

The current situation is illustrated by Figure 9 which shows all operationally Ps bias corrected stations for the 12 UTC analysis cycle on 29 May 2006. There are 1,260 bias corrected stations out 15,444 available stations for this analysis cycle. Furthermore, since the Ps bias correction scheme became operational about 150 biased stations have been taken off the blacklist.

We would like to take this opportunity to thank Anders Persson for his valuable contributions and for bringing the issue of surface-pressure station bias to our attention.

Appendix

The OI adaptive bias correction method

The new bias estimate B_n is found as a linear combination between previously estimated bias B_p and new observation departure D_n so that:

$$B_n = W_p D_n + (1 - W_p) B_p$$

where W_p is the previous bias interpolation weight calculated at the previous observation departure occurrence D_p. The new bias interpolation weight W_n to be used for the next departure occurrence is calculated as:

$$W_n = \frac{\sigma_{bn}^2}{\left(\sigma_{bn}^2 + \sigma_{on}^2\right)}$$

where σ_{bn}^2 and σ_{on}^2 are new bias estimate and observation variances, respectively. They are calculated in a two step procedure. In the first step an intermediate or "guess" bias estimate variance σ_{bg}^2 and observation variance σ_{og}^2 are found from:

$$\sigma_{bg}^2 = \frac{\left[\left(D_n - B_n\right) - \left(D_p - B_p\right)\right]^2}{C}$$

$$\sigma_{og}^2 = \min\left[D_n^2, \left(D_n - B_n\right)^2\right]$$
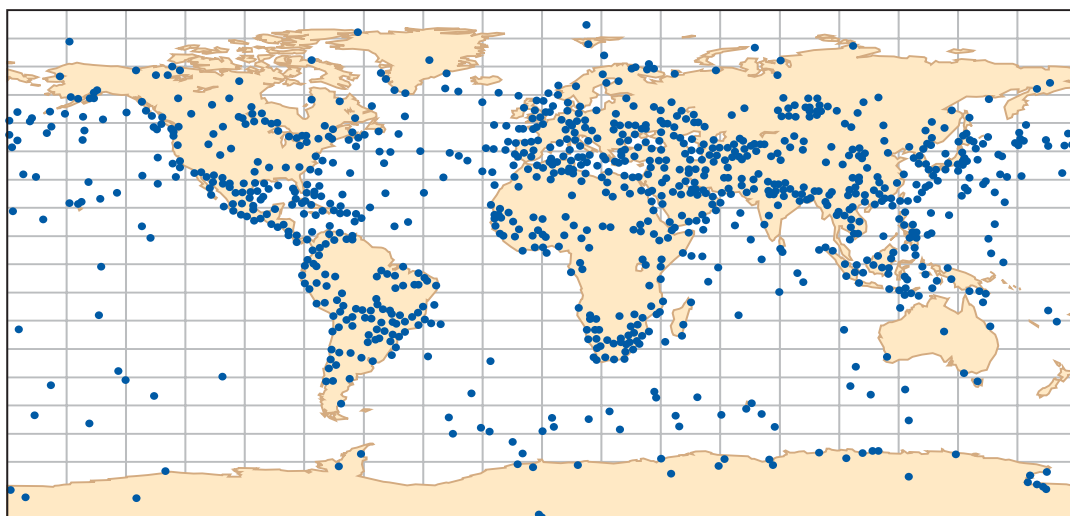
Figure 9 Ps bias corrected stations for the 12 UTC on 29 May 2006 analysis cycle.

where C is a constant (=16). In the second step the final variances are calculated:

$$\sigma_{bn}^2 = W_p \sigma_{bg}^2 + \left(1 - W_p\right)\sigma_{bp}^2$$

$$\sigma_{on}^2 = W_c \sigma_{og}^2 + \left(1 - W_c\right)\sigma_{op}^2$$

where σ_{bp}^2 and σ_{op}^2 are the previous bias estimate and observation variances, and W_c is a constant interpolation weight (=0.010).

ECMWF Calendar 2006/7

2006	
September 4 – 8	Seminar – Polar Meteorology
October 2 – 4	Scientific Advisory Committee (*35th Session*)
October 4 – 6	Technical Advisory Committee (*36th Session*)
October 9 – 13	Meteorological Training Course – Use and interpretation of ECMWF products for WMO Members
October 16 – 17	Finance Committee (*77th Session*)
October 19 – 20	Policy Advisory Committee (*24th Session*)
October 23	Advisory Committee of Co-operating States (*12th Session*)

2006	
October 30 – November 3	Workshop – High performance computing in meteorology (*12th Workshop*)
November 13 – 15	Workshop – Parametrization of clouds in large-scale models
December 4 – 5	Workshop – HALO (*3rd Workshop*)
December 7 – 8	Council (*66th Session*)
2007	
June 28 – 29	Council (*67th Session*)
December 4 – 5	Council (*68th Session*)

ECMWF publications (see http://www.ecmwf.int/publications/)

Technical Memoranda

499 **Buizza**, **R.**, **J-R**. **Bidlot**, **N. Wedi**, **M. Fuentes**, **G. Holt**, **T**. **Palmer** & **F. Vitart**: The new ECMWF Variable Resolution Ensemble Prediction System (VAREPS): methodology and validation. *July 2006*

494 **Lopez**, **P**. & **P. Bauer**: "1D+4D-Var" assimilation of NCEP Stage IV radar and gauge hourly precipitation data. *July 2006*

493 **Andersson**, **E.**, **E. Hólm**, **P. Bauer**, **A. Beljaars**, **G.A.** **Kelly**, **A.P**. **McNally**, **A.J**. **Simmons**, **J.**-N. **Thépaut** &

A.M. **Tompkins**: Analysis and forecast impact of the main humidity observing systems. *June 2006*

491 **Weaver**, **A.T**., **C. Deltel**, **E. Machu**, **S. Ricci** & **N. Daget**: A multivariate balance operator for variational ocean data assimilation. *April 2006*

489 **Benedetti**, **A.** & **M. Fisher**: Background error statistics for aerosols. *June 2006*

Other publications

ECMWF Strategy 2006 – 2015. *August 2006*

Index of past newsletter articles

This is a selection of articles published in the ECMWF Newsletter series during the last five years.
Articles are arranged in date order within each subject category. Articles can be accessed on the ECMWF public web site
www.ecmwf.int/publications/newsletter/index.html

Useful names and telephone numbers within ECMWF

Telephone

Telephone number of an individual at the Centre is:

International: +44 118 949 9 + three digit extension
UK: (0118) 949 9 + three digit extension
Internal: 2 + three digit extension

e.g. the Director's number is:
+44 118 949 9001 (international),
(0118) 949 9001 (UK) and 2001 (internal).

E-mail

The e-mail address of an individual at the Centre is:
firstinitial.lastname@ecmwf.int

e.g. the Director's address is: D.Marbouty@ecmwf.int

For double-barrelled names use a hyphen
e.g. J-N.Name-Name@ecmwf.int

Internet web site

ECMWF's public web site is: http://www.ecmwf.int

	Ext
Director	
Dominique Marbouty	001
Deputy Director & Head of Research Department	
Philippe Bougeault	005
Head of Operations Department	
Walter Zwieflhofer	003
Head of Administration Department	
Ute Dahremöller	005

	Ext
Switchboard	
ECMWF switchboard	000
Advisory	
Internet mail addressed to Advisory@ecmwf.int	
Telefax (+44 118 986 9450, marked User Support)	
Computer Division	
Division Head	
Isabella Weger	050
Computer Operations Section Head	
Sylvia Baylis	301
Networking and Computer Security Section Head	
Matteo Dell'Acqua	356
Servers and Desktops Section Head	
Richard Fisker	355
Systems Software Section Head	
Neil Storer	353
User Support Section Head	
Umberto Modigliani	382
User Support Staff	
Paul Dando	381
Anne Fouilloux	380
Dominique Lucas	386
Carsten Maaß	389
Pam Prior	384
Computer Operations	
Call Desk	303
Call Desk email: cdk@ecmwf.int	
Console - Shift Leaders	803
Console fax number +44 118 949 9840	
Console email: newops@ecmwf.int	
Fault reporting - Call Desk	303
Registration - Call Desk	303
Service queries - Call Desk	303
Tape Requests - Tape Librarian	315

	Ext
Meteorological Division	
Division Head	
Horst Böttger	060
Meteorological Applications Section Head	
Alfred Hofstadler	400
Data and Services Section Head	
Baudouin Raoult	404
Graphics Section Head	
Jens Daabeck	375
Meteorological Operations Section Head	
David Richardson	420
Meteorological Analysts	
Antonio Garcia Mendez	424
Anna Ghelli	425
Claude Gibert (web products)	111
Laura Ferranti (seasonal forecasts)	601
Meteorological Operations Room	426
Data Division	
Division Head	
Adrian Simmons	700
Data Assimilation Section Head	
Erik Andersson	627
Satellite Data Section Head	
Jean-Nöel Thépaut	621
Re-Analysis Project (ERA) Head	
Saki Uppala	366
Probabilistic Forecasting & Diagnostics Division	
Division Head	
Tim Palmer	600
Seasonal Forecasting Section Head	
David Anderson	706
Model Division	
Division Head	
Martin Miller	070
Numerical Aspects Section Head	
Mariano Hortal	147
Physical Aspects Section Head	
Anton Beljaars	035
Ocean Waves Section Head	
Peter Janssen	116
GMES Coordinator	
Anthony Hollingsworth	824
Education & Training	
Renate Hagedorn	257
ECMWF library & documentation distribution	
Els Kooij-Connally	751